

Unnuclear matter at large-charge

Silas R. Beane^{☆✉}, Domenico Orlando^{★☆☆}, and Susanne Reffert^{☆☆}

☆ Albert Einstein Center for Fundamental Physics,
Institute for Theoretical Physics, University of Bern,
Sidlerstrasse 5, CH-3012 Bern, Switzerland

✉ Department of Physics,
University of Washington,
Seattle, WA 98195

★ INFN sezione di Torino.
via Pietro Giuria 1, 10125 Torino, Italy

☆☆ Yukawa Institute for Theoretical Physics, Kyoto University,
Kyoto 650-0047, Japan

The utility of the non-relativistic large-charge effective field theory (EFT) for physical systems, and neutron matter in particular, relies on controlled Schrödinger-symmetry breaking deformations due to scattering length and effective-range effects in the two-body system. A recently-found exact solution of the large-charge system is used to compute these effects for two-point correlation functions of large-charge operators in perturbation theory around the large-charge ground state. Notably, the leading effective-range effects are found to enter at second order in the effective range, in agreement with analogous calculations in the three-body system. The Schrödinger-symmetry breaking deformations are used –together with input from Quantum Monte Carlo simulations– to address the range of validity of the EFT with deformations both in general and in the special case of neutron matter. In particular, it is found that nuclear reactions with up to six low-energy neutrons in the final state can be described by the large-charge EFT with Schrödinger-symmetry breaking.

Contents

1. Introduction	3
2. Fermions near unitarity: EFT definition	6
3. Superfluid EFT	8
3.1. Basics of the Euclidean EFT	8
3.2. Symmetry breaking operators by matching	9
3.3. Energy per particle	9
4. Two-point function at large charge	11
5. First-order range correction	12
5.1. Perturbative expansion defined	12
5.2. EOM in the oscillator frame	14
5.3. Action at the saddle in the flat frame	18
5.4. Boundary effects	20
5.5. Continuity equation and charge conservation	21
6. Second-order effective range correction	23
6.1. EOM in the oscillator frame	23
6.2. Action at the saddle in the flat frame	24
7. Regularization of the two-point function	25
8. Leading-order solution for the scattering length corrections	29
9. Minkowski-space correlation functions	31
9.1. General procedure	31
9.2. Relevant deformations: the scattering length	31
9.3. Irrelevant deformations: effective range	32
10. Unnuclear matter	34
10.1. EFT of neutron matter	34
10.2. Deformation and perturbative window	35
10.3. Three-body example	36
11. Conclusion	37
A. Improved conformal dimension	40
B. Fourier transforms	41

C.	Variation of parameters	41
D.	The boundary term	42
E.	Structure of the solution to the bulk EFT	43

1. Introduction

Recent work [1–4] has demonstrated that certain nuclear reactions with low-energy neutrons in the final state can, in principle, be described by an EFT whose leading order is a nonrelativistic conformal field theory (NRCFT) which describes fermions at unitarity. As scale-invariant matter has no particle interpretation, a field in a NRCFT which describes nuclear matter may be referred to as an “unnucleus”, a non-relativistic analog of the “unparticles” considered in Ref. [5]. As nuclear systems are not Schrödinger invariant, in order to establish the utility of this EFT, it is essential to consider deformations about the unitary fixed point. The s-wave neutron-neutron scattering length is large, and therefore the consequent Schrödinger-symmetry breaking effects should be small at sufficiently small densities and/or momentum transfers. These effects have been computed in Ref. [4] for systems with up to three neutrons in the final state, and it was found that they are indeed small as expected. On the other hand, the neutron-neutron effective range is of natural size, or larger, and therefore one expects that these effects will constitute the dominant symmetry-breaking contribution. For reasons that remain mysterious, the nominally-leading effective-range contributions in three-neutron systems are found to vanish in conformal perturbation theory [4]. Quantification of the effective-range corrections thus requires a more intricate perturbative calculation that has not yet been done in the three-body sector.

Given the inherent complexity of the few-body wave functions, in systems with many neutrons in the final state, it may prove more efficient to work in an EFT which describes the superfluid state of neutron matter [6, 7]. Recent work has shown that correlation functions in this EFT can be computed systematically in a large-charge expansion [8–13], where the conformal dimension of operators is efficiently computed using the state-operator correspondence [14]. Unfortunately, it is not immediately clear how to adapt the state-operator correspondence to account for Schrödinger-symmetry breaking deformations. This renders it challenging to compute the symmetry-breaking contributions to the correlation functions. One of the aims of this work is to show how this can be done systematically.¹

The large-charge expansion [17, 18] is a powerful tool to analytically access strongly-coupled conformal field theories (CFTs) in a sector of large global charge. In very

1. The near-conformal dynamics due to a small dilaton mass in a linear realization of the large-charge EFT has been explored in both the relativistic [15] and non-relativistic [16] cases.

recent work [19], the large-charge master field has been found which allows one to systematically compute all Schrödinger-invariant n-point correlation functions with a single large-charge insertion in the large-charge limit. This solution further allows the simple computation of Schrödinger symmetry breaking corrections in the large-charge EFT due to finite scattering-length effects in the fundamental theory of fermions near unitarity [19]. It is reassuring that at charge $Q = 3$, these results are found to be consistent with the results of Ref. [4] which are computed directly in conformal perturbation theory with the three-body wavefunctions.

This work will consider deformations of Schrödinger symmetry due to effective-range effects, and in addition will consider the general form of the scattering-length and effective-range deformations in a perturbation theory around the large-charge ground state. Perhaps not surprisingly, the nominally-leading effective-range corrections in the large-charge EFT are found to vanish, consistent with the $Q = 3$ result. Therefore, second-order effects in the effective range are computed in perturbation theory.

It may appear that solving the equations of motion (EOM) order-by-order in perturbation theory around the Schrödinger-invariant point is a daunting task; time-translation invariance is broken by the operator insertions, and Schrödinger invariance is explicitly broken by the finite-range corrections. However, the task becomes manageable if a coordinate transformation is applied that corresponds to a frame change in the associated NRCFT, *i.e.* in the undeformed system. For a Schrödinger-invariant system this transformation shifts the insertions to times $\tilde{\tau} = \pm\infty$, preserving the form of the Lagrange density but introducing a background harmonic potential (this is the basis of the non-relativistic state-operator correspondence). In the case at hand, moreover, the Schrödinger-breaking couplings become time-dependent. The resulting system in this *oscillator frame* is non-autonomous, but the EOM simplify, allowing one to find explicit closed-form solutions, which are then transformed back to the initial *flat frame*. In this way one finds an explicit expression for the correlation function, that in energy-momentum space reads

$$\text{Im } G(E, \mathbf{0}) = C_0 E^{\Delta_Q - 5/2} \left[1 + C_Q \left(a \sqrt{ME} \right)^{-1} + C_Q'' r_0^2 ME \right], \quad (1.1)$$

where Δ_Q is the conformal dimension of the lowest operator of charge Q , and C_Q and C_Q'' are known functions of the charge and of the Lagrange-density parameters. While C_Q has been computed in Ref. [19], a primary goal in what follows is to compute C_Q'' .

The large-charge EFT in the Schrödinger limit is a nonrelativistic conformal field theory, and therefore, *a priori*, can be applied only to systems at criticality. However, there is a wide range of physical systems that may be profitably studied using the deformed theory, as the EFT describes all underlying non-relativistic many-body systems that experience superfluidity (*i.e.* the spontaneous breaking of the particle number symmetry) and that

are by some measure near criticality. This is, for example, the case with superfluid atomic gases. Using Feshbach resonances, one can tune the underlying contact forces arbitrarily close to unitarity, and have naturally vanishingly-small effective-range effects and controllable three-body effects. A second example, which is not considered in this paper, is a gas of anyons in $2 + 1$ dimensions which is deformed away from the Schrödinger limit [20].

Of special relevance here are few-body systems of neutrons. Such systems have long been of interest to theorists due to the intriguing possibility of the existence of pure-neutron nuclei². Interest has ramped up recently due to new experimental efforts, particularly at the Radioactive Ion Beam Factory at RIKEN, using the Superconducting Analyzer for Multi-particles from Radio Isotope beams (SAMURAI) [23, 24]. In particular, SAMURAI is able to resolve the energies of the final state neutrons with unparalleled precision. To date reactions with four neutrons in the final state have been studied [25], and systems with six and more final-state neutrons are being explored [24]. The deformed large-charge EFT may provide a valuable tool for computing correlation functions of these systems of low-energy neutrons in the final state of nuclear reactions; i.e. unnuclear matter [1–4].

It is the primary goal of this paper to provide a quantitative answer to the question: how close to unitarity must a system of Q fermions be in order to be profitably described using the deformed large-charge EFT? A corollary of this question relevant to neutron systems is: what is the range of values of Q for which the large-charge EFT provides a systematic, controllable, approximation scheme for describing neutron correlation functions? From the perspective of the fundamental theory of fermions near unitarity, the existence of the large-charge EFT relies on the existence of a well-defined Fermi surface, which in turn implicitly assumes a gas of fermions in the thermodynamic limit. Thus, given the many-body nature of the large-charge EFT, one should expect that the utility of this EFT in describing few-body systems of neutrons will depend critically on the detailed numerical behavior of the perturbative expansion. In any event, answering these questions clearly requires a systematic calculation of the leading symmetry-breaking effects due to scattering length and effective-range effects.

This paper is organized as follows. In Section 2, the underlying EFT of fermions near unitarity is reviewed, and the NRCFT is defined. Section 3 in turn reviews the superfluid EFT which describes fermions near unitarity in the far infrared where the sole active degree of freedom (DOF) is the Goldstone boson of spontaneously broken particle-number symmetry. The symmetry-breaking operators in this EFT are written down, and, via a calculation of the energy density of the system, the coefficients of these operators are shown to be determined by quantum Monte Carlo (MC) simulations of the near-unitary

2. See, for instance, Refs. [21, 22].

Fermi gas. The large-charge EFT in sectors of fixed charge Q is then reviewed in Section 4. Of special importance is the recently discovered master-field solution, which serves as the Schrödinger-invariant Goldstone boson field about which perturbation theory is constructed. Sections 5 and 6 develop perturbation theory to first- and second-order in the effective range, respectively. In computing the large-charge correlation functions, even in the symmetry limit, special attention must be paid to divergences that appear at the boundary of Euclidean time. Section 7 considers various regularization schemes in order to properly separate regularization artifacts from physics. While the leading scattering-length corrections were obtained in Ref. [19], Section 8 recovers these corrections using the new methodology. The final technical steps, continuation back to Minkowski space and Fourier transformation of the correlation functions to energy-momentum space are described in Section 9. Finally, in Section 10 an analysis of the validity of perturbation theory is carried out generally and in the special case of neutron matter. Section 11 summarizes and concludes. In order to relieve the narrative of clutter, some essential material has been organized into a series of appendices.

2. Fermions near unitarity: EFT definition

Consider a system of spin-1/2 fermions which interact via two-body contact forces. At very low energies, where derivative interactions can be ignored, the Lagrange density can be expressed as

$$\mathcal{L} = \psi_\sigma^\dagger \left[i\partial_t + \frac{\vec{\nabla}^2}{2M} \right] \psi_\sigma + \frac{1}{C_0} s^\dagger s + \psi_\downarrow^\dagger \psi_\uparrow^\dagger s + s^\dagger \psi_\uparrow \psi_\downarrow, \quad (2.1)$$

where the field ψ_σ^\dagger creates a fermion of spin $\sigma = \uparrow, \downarrow$, s is an auxiliary field, and C_0 is a bare low-energy constant. In what follows these fermions will be taken to be neutrons. Consider neutron-neutron scattering. Below inelastic thresholds, the s-wave phase shift is given by the effective-range expansion

$$k \cot \delta(k) = -\frac{1}{a} + \frac{1}{2} r_0 k^2 + v_2 k^4 + O(k^6), \quad (2.2)$$

where $k = \sqrt{ME}$ is the on-shell center-of-mass momentum, a is the scattering length, r_0 is the effective range, and v_2 is a shape parameter. In dimensional regularization with the power-divergence subtraction scheme [26, 27] and renormalized at the scale μ , the relation between the low-energy constant C_0 and the scattering length is given by

$$C_0(\mu) = \frac{4\pi}{M} \frac{1}{1/a - \mu}. \quad (2.3)$$

There is a non-trivial ultraviolet (uv) fixed point at $C_0 = C_\star$, corresponding to a divergent scattering length. There is also a trivial fixed point at $C_0 = 0$, corresponding to free particles ($a = 0$). Rescaling the couplings to $\hat{C}_0 \equiv C_0/C_\star$, the beta-function for the rescaled coupling is

$$\hat{\beta}(\hat{C}_0) = \mu \frac{d}{d\mu} \hat{C}_0(\mu) = -\hat{C}_0(\mu) (\hat{C}_0(\mu) - 1), \quad (2.4)$$

which has fixed points at $\hat{C}_0 = 0$ and 1, as shown in Fig. 1. The coupling is near the trivial fixed point for $\mu < 1/|a|$, and near the non-trivial fixed point for $\mu > 1/|a|$.

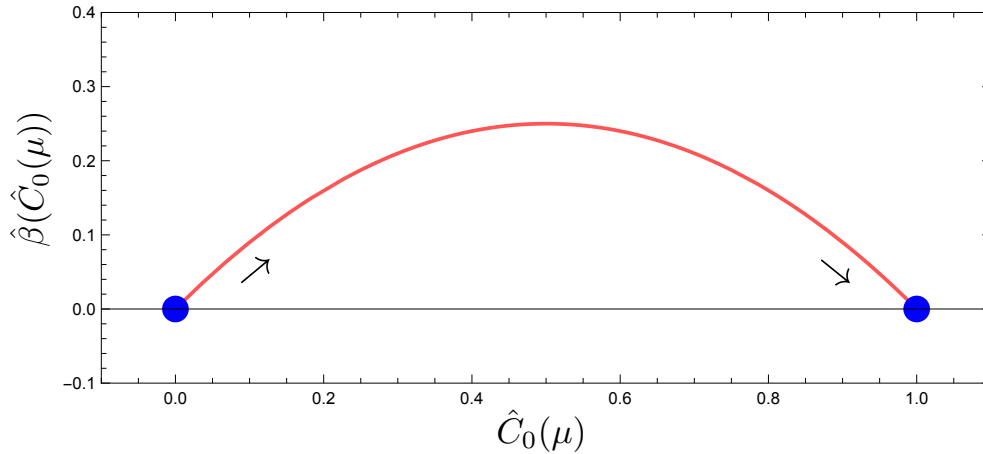


Figure 1 – The beta-function of Eq. (2.4) plotted as a function of $\hat{C}_0(\mu)$. The blue dots are the renormalization group (RG) fixed points. The arrows indicate the direction of increasing μ ; the beta-function curve evolves from $\mu = 0$ (the trivial fixed point) to $\mu = \infty$ (the unitary fixed point).

Expanding about the uv fixed point, the system of low-energy fermions is described by a NRCFT, defined by the Lagrange density

$$\mathcal{L}_{\text{CFT}} = \psi_\sigma^\dagger \left[i\partial_t + \frac{\vec{\nabla}^2}{2M} \right] \psi_\sigma + \frac{1}{C_\star} s^\dagger s + \psi_\downarrow^\dagger \psi_\uparrow^\dagger s + s^\dagger \psi_\uparrow \psi_\downarrow. \quad (2.5)$$

Consider now the inclusion of small Schrödinger-breaking effects in the fundamental theory. Using Eq. (2.1) and Eq. (2.3) one can write

$$\mathcal{L} = \mathcal{L}_{\text{CFT}} + \frac{M}{4\pi a} s^\dagger s - \frac{M^2 r_0}{8\pi} s^\dagger \left(i\overleftrightarrow{\partial}_t + \frac{\vec{\nabla}^2 + \overleftarrow{\nabla}^2}{4M} \right) s, \quad (2.6)$$

where, in addition, effective-range corrections have been included [4, 28]. Note that the field ψ_σ has conformal dimension 3/2 while the field s at unitarity has conformal dimen-

sion 2 [14]. The scattering length corrections therefore enter via a relevant dimension-4 operator, and the effective-range corrections enter via an irrelevant dimension-6 operator. Therefore, the operators are formally scale invariant if a^{-1} and r are assigned conformal dimensions 1 and -1 , respectively.

3. Superfluid EFT

3.1. Basics of the Euclidean EFT

Many neutrons at and near unitarity are superfluid and therefore are described in the infrared (IR) by an EFT of the Goldstone boson, $\theta(x)$, of spontaneously broken particle number [6, 7]. In Euclidean space, the partition function is

$$Z = \int \mathcal{D}\theta \exp(-S) = \int \mathcal{D}\theta \exp\left(-\int d\tau d^3x \mathcal{L}\right), \quad (3.1)$$

where, at LO,

$$\mathcal{L}_{\text{LO}} = -c_0 M^{3/2} X^{5/2}, \quad (3.2)$$

with

$$X = i\partial_\tau\theta - \frac{(\partial_i\theta)^2}{2M}. \quad (3.3)$$

One readily checks that \mathcal{L}_{LO} is Schrödinger invariant and therefore defines a NRCFT [6, 7]. The density and Hamiltonian density are given by, respectively,

$$\rho = -\frac{\delta\mathcal{L}}{\delta X}, \quad \mathcal{H} = \mathcal{L} - \dot{\theta}\frac{\partial\mathcal{L}}{\partial\dot{\theta}}, \quad (3.4)$$

where $\dot{\theta} \equiv \partial_\tau\theta$. The Euler-Lagrange equations take the form

$$\partial_\tau\rho + \frac{1}{M}\partial_i(i\partial_i\theta\rho) = 0. \quad (3.5)$$

At LO, one finds the solution³

$$\theta = -i\mu\tau, \quad X = \mu, \quad (3.6)$$

which describes the homogeneous ground state of the system.

3. From this equation forward, μ denotes the chemical potential.

3.2. Symmetry breaking operators by matching

As the Goldstone field X carries conformal dimension 2, a spurion analysis gives the leading symmetry-breaking operators in the superfluid EFT,

$$\mathcal{L}_{\text{SB}} = -g_1 a^{-1} M X^2 - g_2 a^{-2} M^{1/2} X^{3/2} - h_1 r_0 M^2 X^3 - h_2 r_0^2 M^{5/2} X^{7/2} + \dots, \quad (3.7)$$

where the g_i and the h_i are dimensionless constants.⁴ Here it is assumed that the scattering length and effective range effects are tuned independently; i.e., no mixed operators are considered. The ordering of these operators within the large-charge EFT will be considered in detail below. Note that shape parameter corrections enter at $\mathcal{O}(r_0^3)$ and therefore will not be considered in this work. In the homogeneous ground state, with $M = 1$, the grand-canonical potential is read off from the total Lagrange density as:

$$\Omega(\mu) = -c_0 \mu^{5/2} - g_1 a^{-1} \mu^2 - g_2 a^{-2} \mu^{3/2} - h_1 r_0 \mu^3 - h_2 r_0^2 \mu^{7/2} + \dots \quad (3.8)$$

The constants g_i and the h_i are numbers of order unity which determine quantitatively the leading effects of the deformation of Schrödinger symmetry due to finite a and non-vanishing r_0 . As will be shown in the next section, these numbers have been determined using quantum MC simulations.

3.3. Energy per particle

Using dimensional analysis to write down deformations away from unitarity, the energy-per-particle E/N of the interacting Fermi gas in the near-Schrödinger limit can be written at very-low densities as [29–31]

$$E/N = \frac{3}{5} \frac{k_F^2}{2M} \left(\xi - \frac{\zeta}{k_F a} - \frac{\zeta_2}{k_F^2 a^2} + \dots + \eta k_F r_0 + \eta_2 k_F^2 r_0^2 + \dots \right). \quad (3.9)$$

Here the various dimensionless universal parameters have been determined using quantum MC simulations. From Ref. [29], $\xi = 0.372(5)$ (Bertsch parameter) and $\eta = 0.12(3)$. The quadratic range corrections have been studied in Ref. [32]; the average of two determinations gives $\eta_2 = -0.03(2)$. From the simulation data in Ref. [33], it is straightforward to extract $\zeta = -0.68(15)$ and $\zeta_2 = 3.6(10)$. For the case of neutron matter, at densities corresponding to interparticle separations greater than the pion Compton wavelength, the energy-per-particle with the quantum MC determination of the deformation away from unitarity is shown in Fig. 2.

It is straightforward to obtain Eq. (3.9) in the superfluid EFT. The energy density can

4. Note that this is the Euclidean Lagrange density, while the constants have been defined with a plus sign in Minkowski space. The parameters $g_{1,2}$, defined in Ref. [19], differ by an overall sign.

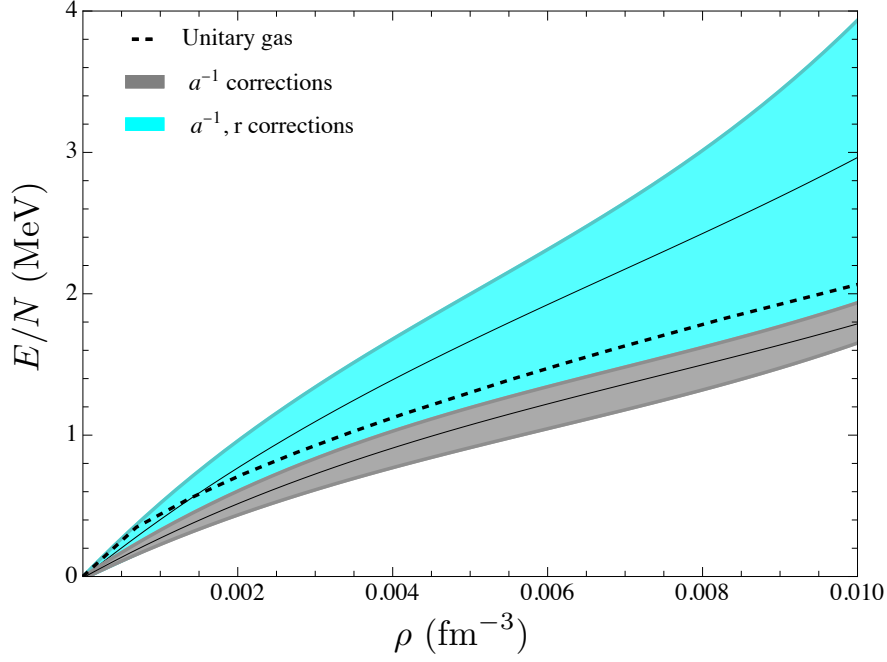


Figure 2 – Energy per particle in neutron matter at low densities, as taken from Eq. (3.9). The error bands are from propagation of the quantum MC uncertainties.

be obtained from the grand-canonical potential by the (Euclidean) Legendre transform,

$$\Omega(\mu) = \mathcal{E}(\mu) + \mu\rho . \quad (3.10)$$

Note that while the density ρ is fixed in terms of k_F , the chemical potential μ is shifted away from the Fermi energy by the symmetry-breaking effects. That is,

$$\rho = \frac{k_F^3}{3\pi^2} = -\frac{\delta\Omega(\mu)}{\delta\mu} . \quad (3.11)$$

One then finds Eq. (3.9) with

$$c_0 = \frac{2^{5/2}}{15\pi^2\xi^{3/2}} = 0.168(3) , \quad (3.12)$$

$$g_1 = \frac{2\zeta}{5\pi^2\xi^2} = -0.20(4) , \quad g_2 = \frac{\sqrt{2}}{25\pi^2\xi^{5/2}} \left(4\zeta^2 + 5\zeta_2\xi \right) = 0.58(6) , \quad (3.13)$$

$$h_1 = \frac{4\eta}{5\pi^2\xi^3} = 0.19(5) , \quad h_2 = \frac{4\sqrt{2}}{25\pi^2\xi^{9/2}} \left(9\eta^2 - 5\eta_2\xi \right) = 0.38(15) . \quad (3.14)$$

These values of the universal constants will be used below in the quantitative determination of the deformed correlation functions.

4. Two-point function at large charge

This section briefly reviews the main developments of Ref. [19] as this provides the basis of the perturbation theory that follows. In the large-charge EFT, the charge- Q primary operator of conformal dimension Δ is

$$O_{\Delta,Q} = \mathcal{N} X^{\Delta/2} \exp(iQ\theta), \quad (4.1)$$

where \mathcal{N} is a normalization constant. The two-point function which evolves superfluid matter of charge Q and *a priori* unknown conformal dimension Δ from source point x_2 to source point x_1 in the Schrödinger limit, is defined via the path integral

$$G_Q(x_1; x_2) = G_Q(\tau_1, \mathbf{x}_1; \tau_2, \mathbf{x}_2) = \int \mathcal{D}\theta O_{\Delta,Q}(x_2) O_{\Delta,-Q}(x_1) e^{-\int d^4x \mathcal{L}_{\text{LO}}}. \quad (4.2)$$

Schrödinger symmetry completely constrains the two-point function to be of the form [34–36]

$$G_Q(x_1, x_2) = \mathcal{N}^2 \tau_{12}^{-\Delta} \exp\left(-\frac{QM\mathbf{x}_{12}^2}{2\tau_{12}}\right), \quad (4.3)$$

where $\tau_{12} \equiv \tau_1 - \tau_2$, $\mathbf{x}_{12} \equiv \mathbf{x}_1 - \mathbf{x}_2$. In the presence of sources, the EOM acquires a source term so that

$$\partial_{\tau}\rho + \frac{1}{M}\partial_i(i\partial_i\theta\rho) = Q[\delta^4(\mathbf{x} - \mathbf{x}_2) - \delta^4(\mathbf{x} - \mathbf{x}_1)]. \quad (4.4)$$

The master-field solution to the EOM and the saddle point location in the presence of sources is given by [19, 37]

$$\theta_s(\tau, \mathbf{x}|\tau_1, \mathbf{x}_1; \tau_2, \mathbf{x}_2) = \frac{i}{2}\gamma \log\left(\frac{\tau_1 - \tau}{\tau - \tau_2}\right) - \frac{i}{4}\left[\frac{(\mathbf{x} - \mathbf{x}_2)^2}{(\tau - \tau_2)} - \frac{(\mathbf{x} - \mathbf{x}_1)^2}{(\tau_1 - \tau)}\right], \quad (4.5)$$

where the anomalous dimension γ is

$$\gamma = \frac{\mu}{2}\tau_{12} = 3^{1/3}\xi^{1/2}Q^{1/3}. \quad (4.6)$$

Now the two-point function evaluated at the master-field solution is

$$G_Q(x_1, x_2) = \lim_{\epsilon \rightarrow 0} O_{\Delta,Q}(\tau_2 + \epsilon, \mathbf{x}_2) O_{\Delta,-Q}(\tau_1 - \epsilon, \mathbf{x}_1) \exp\left[-\int_{\tau_2 + \epsilon}^{\tau_1 - \epsilon} d\tau \int d^3\mathbf{x} \mathcal{L}_{\text{LO}}[\theta]\right] \Bigg|_{\theta = \theta_s}, \quad (4.7)$$

where the temporal boundaries have been shifted by ϵ . The existence of the $\epsilon \rightarrow 0$ limit provides a constraint that is used to compute the conformal dimension Δ [19].

One finds at the saddle,

$$S_{\text{SB}}[\theta_s] = -\frac{3^{1/3}\xi^{1/2}}{4}Q^{4/3}\log\left(\frac{\tau_{12}}{\epsilon}\right). \quad (4.8)$$

Substituting the saddle solution into the expression for the operators one then finds

$$G_Q(x_1; x_2) \sim \epsilon^{Q\gamma - \Delta - \frac{3^{1/3}\xi^{1/2}}{4}Q^{4/3}} \tau_{12}^{-Q\gamma + \frac{3^{1/3}\xi^{1/2}}{4}Q^{4/3}} e^{-\frac{QMx_{12}^2}{2\tau_{12}}}. \quad (4.9)$$

Finally, absence of the divergence for $\epsilon \rightarrow 0$ determines the conformal dimension

$$\Delta_Q = Q\gamma - \frac{3^{1/3}\xi^{1/2}}{4}Q^{4/3} = \frac{3^{4/3}}{4}\xi^{1/2}Q^{4/3}, \quad (4.10)$$

in agreement with the state-operator correspondence [9].

The goal of this paper is to perturbatively compute the leading symmetry-breaking corrections to this correlation function, with

$$\mathcal{L}[\theta] = \mathcal{L}_{\text{LO}}[\theta] + \mathcal{L}_{\text{SB}}[\theta]. \quad (4.11)$$

Naively, the leading symmetry-breaking corrections are evaluated by computing the symmetry-breaking action at the saddle-point solution. For instance, for the two-point function, one expects

$$G(x_1; x_2) = G_Q(x_1; x_2)e^{-S_{\text{SB}}[\theta_s]}. \quad (4.12)$$

While in practice this gives the correct result for the scattering-length corrections [19], in general this procedure fails, as there are non-vanishing boundary terms in the effective action which must be included. A simple example of an action whose perturbative expansion contains boundary terms is provided in Appendix D.

5. First-order range correction

5.1. Perturbative expansion defined

This section aims to describe the effect of a finite effective interaction range r_0 on the form of the two-point function. The approach is perturbative, and one begins with the Lagrange density

$$\mathcal{L} = -c_0X^{5/2} - h_1r_0X^3 - h_2r_0^2X^{7/2} + \dots. \quad (5.1)$$

First, the parametric range of validity of the approximation should be established. At the saddle solution, Eq. (4.5), corresponding to the insertion of two operators at distance

τ_{12} in the temporal direction, the operator $X_{\otimes} \equiv X[\theta_s]$ scales as $X_{\otimes} = \mathcal{O}(\mu) = \mathcal{O}(\gamma/\tau_{12})$. Thus, the r_0 term can be treated perturbatively as long as

$$r_0\sqrt{\mu} = r_0\sqrt{\frac{\gamma}{\tau_{12}}} \ll 1. \quad (5.2)$$

A hierarchy with respect to Schrödinger-invariant corrections to Eq. (5.1) should also be established. One may assume, for instance, that the leading effective-range corrections are much larger than the first subleading correction in the large-charge expansion of the pure Schrödinger system. It is known [7, 38] that this latter correction is suppressed by $1/\gamma^2$ with respect to the c_0 term. Therefore, in addition one has

$$r_0\sqrt{\mu} = r_0\sqrt{\frac{\gamma}{\tau_{12}}} \gg \frac{1}{\gamma^2}. \quad (5.3)$$

Using the fact that $\gamma = \mathcal{O}(Q^{1/3})$, it then follows that the effective range in units of τ_{12} should satisfy

$$\frac{1}{Q^{5/6}} \ll \frac{r_0}{\sqrt{\tau_{12}}} \ll \frac{1}{Q^{1/6}}. \quad (5.4)$$

It will be seen below that the first non-vanishing correction due to the effective range is of order r_0^2 , and, therefore, by the same argument one has

$$\frac{1}{Q} \ll \frac{r_0^2}{\tau_{12}} \ll \frac{1}{Q^{1/3}}. \quad (5.5)$$

Hence, formally, the perturbative expansion developed below treats the limit $r_0 \rightarrow 0$, $\mu \rightarrow \infty$ with the product $r_0\sqrt{\mu} \equiv \kappa$ held fixed and small.

An analogous analysis applies in consideration of the perturbation theory with a finite scattering length a . In this case, a consistent hierarchy is

$$\frac{1}{Q^{1/2}} \ll \frac{\sqrt{\tau_{12}}}{a} \ll Q^{1/6}, \quad (5.6)$$

where formally, the perturbative expansion treats the limit $a \rightarrow \infty$, $\mu \rightarrow \infty$ with the product $a^{-1}\sqrt{\mu}$ held fixed and small. The leading symmetry-breaking corrections due to a finite scattering length were obtained in Ref. [19], and a generalization of this solution will be discussed below.

5.2. EOM in the oscillator frame

The goal is to perturbatively compute the two-point function with Schrödinger-symmetry breaking; *i.e.*

$$G_Q(x_1; x_2) = \int \mathcal{D}\theta \mathcal{O}_{\Delta, Q}(x_2) \mathcal{O}_{\Delta, -Q}(x_1) e^{-\int d^4x \mathcal{L}}, \quad (5.7)$$

with the Lagrange density given in Eq. (5.1). While this Lagrange density breaks scale and conformal invariance, it preserves Galilean invariance (including translations and rotations) since the symmetry-breaking operators commute with Galilean boosts. It follows that the two-point function of primary operators must take the form [4, 36]

$$G_Q(x_1; x_2) = f(\tau_{12}) \exp\left(-\frac{Qx_{12}^2}{2\tau_{12}}\right), \quad (5.8)$$

where f is an arbitrary function. Hence, the dependence on the spatial component of the insertions is completely fixed in the deformed theory. Because of this, in the following one can specialize to the simpler case where operator insertions are taken at $\mathbf{x}_1 = \mathbf{x}_2 = 0$ and $\tau_1 = 1/\omega$, $\tau_2 = -1/\omega$.

The strategy is then to compute the semiclassical field configuration $\theta(\tau, \mathbf{x} | -1/\omega, 0; 1/\omega, 0)$ resulting from the insertions. This choice does not result in any loss of generality. Since the deformed system retains Galilean invariance, the field configuration corresponding to generic insertions may be obtained using a Galilean boost that maps $(-1/\omega, 0)$ into (τ_2, \mathbf{x}_2) and $(1/\omega, 0)$ into (τ_1, \mathbf{x}_1) (see *e.g.* [8] for the transformation properties of θ):

$$\theta(\tau, \mathbf{x} | \tau_2, \mathbf{x}_2; \tau_1, \mathbf{x}_1) = \theta\left(\tau + \frac{\tau_1 + \tau_2}{2}, \mathbf{x} + \omega\tau \frac{\mathbf{x}_1 - \mathbf{x}_2}{2} + \frac{\mathbf{x}_1 + \mathbf{x}_2}{2} \mid -1/\omega, 0; 1/\omega, 0\right) + \frac{i\omega}{2}(\mathbf{x}_1 - \mathbf{x}_2) \cdot \left(\mathbf{x} - \frac{\omega\tau}{4}(\mathbf{x}_1 - \mathbf{x}_2)\right). \quad (5.9)$$

Even with the simplified source locations, the EOM in the presence of symmetry breaking is highly complex. A fruitful idea is to map the problem to a different frame where the EOM become tractable, and then revert to the original frame. As explained above, the focus will be on the case $\mathbf{x}_1 = \mathbf{x}_2 = 0$, and $\tau_1 = -1/\omega$ and $\tau_2 = 1/\omega$. This choice is convenient because then one can transform to the oscillator frame, where the insertions are at $\tilde{\tau} = \pm\infty$. The relevant change of variables is given in [19, 39]:

$$\begin{cases} \omega\tau = \tanh(\omega\tilde{\tau}) \\ \mathbf{x} = \frac{\tilde{\mathbf{x}}}{\cosh(\omega\tilde{\tau})} \end{cases}, \quad \begin{cases} \omega\tilde{\tau} = \operatorname{arctanh}(\omega\tau) \\ \tilde{\mathbf{x}} = \frac{\mathbf{x}}{\sqrt{1-\omega^2\tau^2}} \end{cases}, \quad \theta(\tau, \mathbf{x}) = \tilde{\theta}(\tilde{\tau}, \tilde{\mathbf{x}}) - \frac{i}{4} \left(\frac{x^2}{\tau + 1/\omega} + \frac{x^2}{\tau - 1/\omega} \right). \quad (5.10)$$

Consider the Lagrange density with the nominally leading effective-range corrections. The $X^{5/2}$ term is Schrödinger invariant, while the X^3 term is not, and therefore in the

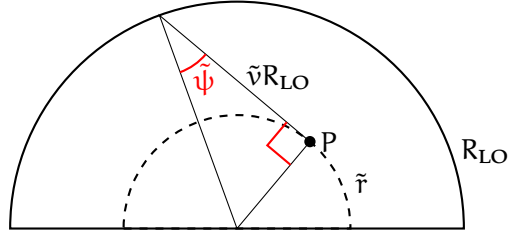


Figure 3 – The angle $\tilde{\psi}$ identifies points P at distance \tilde{r} from the center of the droplet (dashed circle). $\tilde{\psi} = 0$ is the center of the drop and $\tilde{\psi} = \pi/2$ is the LO edge, where the triangle degenerates into a segment.

oscillator frame the Lagrange density reads

$$\tilde{\mathcal{L}} = c_0 \tilde{X}^{5/2} + r_0 h_1 \cosh(\omega \tilde{\tau}) \tilde{X}^3, \quad (5.11)$$

where now

$$\tilde{X} = i \partial_{\tilde{\tau}} \tilde{\theta} - \frac{\omega^2 \tilde{x}^2}{2} - \frac{1}{2} (\partial_i \tilde{\theta})^2. \quad (5.12)$$

Note that the symmetry-breaking term has a time-dependent coupling (the Hamiltonian system is non-autonomous).

The eom has the same form as for $r_0 = 0$, since the Lagrangian depends on $\tilde{\theta}$ only via \tilde{X} :

$$i \partial_{\tilde{\tau}} \frac{\delta \tilde{\mathcal{L}}}{\delta \tilde{X}} - \partial_i \left(\partial_i \tilde{\theta} \frac{\delta \tilde{\mathcal{L}}}{\delta \tilde{X}} \right) = 0. \quad (5.13)$$

Now consider isotropic solutions, depending only on $\tilde{x} = |\tilde{\mathbf{x}}|$, and introduce the variable

$$\tilde{v}^2 = 1 - \frac{\omega^2}{2\mu} \tilde{x}^2 = 1 - \frac{\tilde{x}^2}{R_{\text{LO}}^2}, \quad (5.14)$$

where R_{LO} is the size of the droplet at LO [7, 38], which is spanned by $0 < \tilde{v} < 1$, where $\tilde{v} = 1$ is the center and $\tilde{v} = 0$ the border. In the following it will be convenient to rewrite \tilde{v} in terms of an angular variable $\tilde{v} = \cos(\tilde{\psi})$. The distance from the center of the droplet is $\tilde{r} = |\tilde{\mathbf{x}}| = R_{\text{LO}} \sin(\tilde{\psi})$, and it is apparent that $\tilde{\psi} = 0$ is the center, and $\tilde{\psi} = \pi/2$ is the LO edge (see Fig. 3). As it will be necessary to integrate over the droplet, it is useful to express the volume element in the various coordinates:

$$d^3 \tilde{\mathbf{x}} = d\Omega \tilde{r}^2 d\tilde{r} = -R_{\text{LO}}^3 d\Omega \sqrt{1 - \tilde{v}^2} \tilde{v} d\tilde{v} = R_{\text{LO}}^3 d\Omega \sin^2(\tilde{\psi}) \cos(\tilde{\psi}) d\tilde{\psi}, \quad (5.15)$$

where $d\Omega$ is the measure over the two-sphere.

It is convenient to express the $O(r_0)$ solution in the form

$$\tilde{\theta}(\tilde{\tau}, \tilde{\nu}) = \tilde{\theta}_0(\tilde{\tau}, \tilde{\nu}) + \frac{\mu^{3/2}}{\omega} r_0 \tilde{\theta}_1(\tilde{\tau}, \tilde{\nu}) \quad (5.16)$$

and expand the EOM to first order in $\mu^{1/2}r_0 \ll 1$. The problem has three dimensional quantities, r_0 , μ and ω , from which one obtains two dimensionless ones $\mu^{1/2}r_0$ and μ/ω .

Recall that the leading-order solution is

$$\tilde{\theta}_0(\tau, \tilde{\nu}) = -i\mu\tilde{\tau} \quad (5.17)$$

and the $O(\mu^{1/2}r_0)$ EOM takes the simple form

$$\frac{3\tilde{\nu}}{\omega^2} \frac{\partial^2}{\partial \tilde{\tau}^2} \tilde{\theta}_1 + \tilde{\nu}(1 - \tilde{\nu}^2) \tilde{\theta}_1'' + (2 - 5\tilde{\nu}^2) \tilde{\theta}_1' = \frac{12h_1 i}{5c_0} \tilde{\nu}^4 \sinh(\omega\tilde{\tau}), \quad (5.18)$$

where $\tilde{\theta}_1' = \partial_{\tilde{\nu}} \tilde{\theta}_1$. This is a linear inhomogeneous partial differential equation (PDE). The standard approach is to look for a particular solution $\tilde{\theta}_{1,p}$ and then solve the associated homogeneous equation to find the general solution to the problem.

One can use separation of variables, observing that the inhomogeneity is proportional to $\sinh(\omega\tilde{\tau})$. It follows that

$$\tilde{\theta}_{1,p}(\tilde{\tau}, \tilde{\nu}) = i \frac{h_1}{c_0} \sinh(\omega\tilde{\tau}) B_1(\tilde{\nu}) \quad (5.19)$$

which leads to an inhomogeneous ordinary differential equation (ODE) for $B_1^p(\tilde{\nu})$:

$$\tilde{\nu}(1 - \tilde{\nu}^2) B_1'' + (2 - 5\tilde{\nu}^2) B_1' + 3\tilde{\nu} B_1 = \frac{12i}{5} \tilde{\nu}^4. \quad (5.20)$$

The source is an elementary function of $\tilde{\nu}$, and therefore a standard variation of parameters⁵ leads to

$$B_1(\tilde{\nu}) = -\frac{2}{15} \left(\tilde{\nu}^3 + 6\tilde{\nu} - \frac{2}{\tilde{\nu}} \right). \quad (5.21)$$

Now that the particular solution is in hand, one is left with solving the associated homogeneous problem:

$$\frac{3\tilde{\nu}}{\omega^2} \frac{\partial^2}{\partial \tilde{\tau}^2} \tilde{\theta}_h + \tilde{\nu}(1 - \tilde{\nu}^2) \tilde{\theta}_h'' + (2 - 5\tilde{\nu}^2) \tilde{\theta}_h' = 0. \quad (5.22)$$

Again searching for a solution by separating the variables,

$$\tilde{\theta}_h(\tilde{\tau}, \tilde{\nu}) = A(\omega\tilde{\tau}) C(\tilde{\nu}), \quad (5.23)$$

5. This method is reviewed in Appendix C.

the homogeneous equation becomes

$$\frac{\ddot{A}(\omega\tilde{\tau})}{A(\omega\tilde{\tau})} = \frac{(5\tilde{v}^2 - 2)C'(\tilde{v}) + \tilde{v}(\tilde{v}^2 - 1)C''(\tilde{v})}{3\tilde{v}C(\tilde{v})} \quad (5.24)$$

which admits the solution

$$A(\omega\tilde{\tau}) = c_1 e^{\lambda\omega\tilde{\tau}} + c_2 e^{-\lambda\omega\tilde{\tau}}, \quad (5.25)$$

$$\begin{aligned} C(\tilde{v}) &= k_1 \frac{\cos\left(\sqrt{4+3\lambda^2}\arccos(\tilde{v})\right)}{\tilde{v}\sqrt{1-\tilde{v}^2}} + k_2 \frac{\sin\left(\sqrt{4+3\lambda^2}\arccos(\tilde{v})\right)}{\tilde{v}\sqrt{1-\tilde{v}^2}} \\ &= \frac{k_1 \cos\left(\sqrt{4+3\lambda^2}\tilde{\psi}\right) + k_2 \sin\left(\sqrt{4+3\lambda^2}\tilde{\psi}\right)}{\sin(\tilde{\psi})\cos(\tilde{\psi})}, \end{aligned} \quad (5.26)$$

where the last step has implemented the change of variables described above.

Putting the two elements together leads to the general solution of the problem:

$$\begin{aligned} \tilde{\theta}_1(\tilde{\tau}, \tilde{v}) &= -\frac{2h_1 i}{15c_0} \left(\tilde{v}^3 + 6\tilde{v} - \frac{2}{\tilde{v}} \right) \sinh(\omega\tilde{\tau}) + \left(c_1 e^{\lambda\omega\tilde{\tau}} + c_2 e^{-\lambda\omega\tilde{\tau}} \right) \\ &\quad \left(k_1 \frac{\cos\left(\sqrt{4+3\lambda^2}\tilde{\psi}\right)}{\sin(\tilde{\psi})\cos(\tilde{\psi})} + k_2 \frac{\sin\left(\sqrt{4+3\lambda^2}\tilde{\psi}\right)}{\sin(\tilde{\psi})\cos(\tilde{\psi})} \right). \end{aligned} \quad (5.27)$$

The next step is the imposition of boundary conditions. First, note that the system has opposite insertions at $\tilde{\tau} = \pm\infty$, which selects solutions that are odd under $\tilde{\tau} \rightarrow -\tilde{\tau}$, fixing $c_1 = -c_2 = 1/2$ (for convenience). As for the dependence on \tilde{v} , the coefficient of the highest derivative term in the PDE vanishes for $\tilde{v} = 0$ and $\tilde{v} = 1$. It follows that the general solution is singular both in $\tilde{v} = 0$ and $\tilde{v} = 1$. For $\tilde{\psi} \sim 0$ (center of the droplet $\tilde{v} = 1$), one has

$$\tilde{\theta}_1(\tilde{\tau}, \tilde{v}) \underset{\tilde{\psi} \rightarrow 0}{\sim} \frac{k_1}{\tilde{\psi}} \sinh(\lambda\omega\tilde{\tau}) + \text{regular}. \quad (5.28)$$

There is no physical reason to expect a singularity at the center of the droplet, and therefore $k_1 = 0$. At the edge, however, the situation is different. Already at LO, before any perturbation is considered, the large-charge approximation is not strictly valid since the charge density goes to zero [7]. So there is no reason to trust the solution at the droplet edge and impose regularity. Instead, the remaining parameters are fixed by minimizing the energy and then considering in detail the consequences of the (singular) behavior of \tilde{X} around the LO edge $\tilde{\psi} = \psi_{\text{LO}} = \pi/2$, in order to show that the corresponding corrections are parametrically suppressed.

At leading order in r_0 ,

$$\tilde{X}(\tilde{\tau}, \tilde{\psi}) = \mu \cos^2(\tilde{\psi}) - \frac{r_0 \mu^{3/2} h_1}{c_0} B_1(\tilde{\nu}) \cosh(\omega \tilde{\tau}) + r_0 \mu^{3/2} k_2 \lambda \frac{\sin(\sqrt{4 + 3\lambda^2} \tilde{\psi})}{\sin(\tilde{\psi}) \cos(\tilde{\psi})} \cosh(\lambda \omega \tau), \quad (5.29)$$

so that the Lagrange density at the saddle is

$$\begin{aligned} \tilde{\mathcal{L}}_{\text{eff}} = & -c_0 \mu^{5/2} \cos^5(\tilde{\psi}) - h_1 r_0 \mu^3 \cos^6(\tilde{\psi}) \cosh(\omega \tilde{\tau}) \\ & - \frac{5}{2} c_0 r_0 \mu^3 \cos^3(\tilde{\psi}) \left(\frac{h_1}{c_0} B_1(\tilde{\nu}) \cosh(\omega \tilde{\tau}) + k_2 \lambda \frac{\sin(\sqrt{4 + 3\lambda^2} \tilde{\psi})}{\sin(\tilde{\psi}) \cos(\tilde{\psi})} \cosh(\lambda \omega \tau) \right). \end{aligned} \quad (5.30)$$

The action now takes the form

$$\begin{aligned} \tilde{S}_{\text{eff}} = & \int_{-\infty}^{\infty} d\tilde{\tau} \int d^3\tilde{\chi} \tilde{\mathcal{L}}_{\text{eff}} = 4\pi R_{\text{LO}}^3 \int_{-T}^T d\tilde{\tau} \int_0^{\pi/2} \sin^2(\tilde{\psi}) \cos(\tilde{\psi}) d\tilde{\psi} \tilde{\mathcal{L}}_{\text{eff}} \\ = & -\frac{5\pi^2 c_0 T}{8\sqrt{2}} \frac{\mu^4}{\omega^3} \left[1 - h_1 r_0 \sqrt{\mu} \left(\frac{31744}{4725} \frac{\sinh(\omega T)}{\omega T c_0} + k_2 \frac{256 \sin(\frac{\pi}{2} \sqrt{4 + 3\lambda^2}) \sinh(\lambda \omega T)}{3\pi \lambda^2 (4 - \lambda^2) \omega T} \right) \right], \end{aligned} \quad (5.31)$$

which is minimized for $k_2 = 0$. (Note that for arbitrary $\lambda > 2$, in the continuation back to Minkowski space, the k_2 term correspond to higher harmonics which incur an energy cost.)

The final result is that the lowest-energy configuration at next-to-leading order (NLO) in the effective range in the oscillator frame is

$$\tilde{\theta}(\tilde{\tau}, \tilde{\nu}) = -i\mu \tilde{\tau} + i \frac{h_1}{c_0} \frac{r_0 \mu^{3/2}}{\omega} B_1(\tilde{\nu}) \sinh(\omega \tilde{\tau}). \quad (5.32)$$

5.3. Action at the saddle in the flat frame

The next step is to move to the flat frame. The transformations of θ and the kinematical variables are given in Eq. (5.10), and

$$\tilde{v}^2 = 1 - \frac{\tilde{r}^2}{R_{\text{LO}}^2} \mapsto v^2 = 1 - \frac{r^2}{R_{\text{LO}}^2 (1 - \omega^2 \tau^2)} \quad (5.33)$$

$$\sin(\tilde{\psi}) = \frac{\tilde{r}}{R_{\text{LO}}} \mapsto \sin(\psi) = \frac{r}{R_{\text{LO}} (1 - \omega^2 \tau^2)^{1/2}}. \quad (5.34)$$

The volume form is then

$$\begin{aligned} d\tau d^3\chi &= r^2 dr d\tau d\Omega = -R_{\text{LO}}^3 (1 - \omega^2 \tau^2)^{3/2} \sqrt{1 - v^2} v dv d\tau d\Omega \\ &= R_{\text{LO}}^3 (1 - \omega^2 \tau^2)^{3/2} \sin^2(\psi) \cos(\psi) d\psi d\tau d\Omega. \end{aligned} \quad (5.35)$$

Finally, the solution in the flat frame is

$$\theta(\tau, v) = \frac{i\mu}{2\omega} \log \frac{1 - \omega\tau}{1 + \omega\tau} + i(1 - v^2)\mu\tau + i\frac{h_1}{c_0} r_0 \mu^{3/2} \frac{\tau}{\sqrt{1 - \omega^2 \tau^2}} B_1(v) \quad (5.36)$$

with the corresponding value of χ ,

$$\chi(\tau, v) = \frac{v^2 \mu}{1 - \omega^2 \tau^2} - r_0 \frac{h_1}{c_0} \left(\frac{\mu}{1 - \omega^2 \tau^2} \right)^{3/2} B_1(v). \quad (5.37)$$

χ diverges at the droplet edge due to the divergence in B_1 which scales like $1/v$. This is, however, not an issue, as this divergence cancels out in the density. Expanding ρ to leading order in r_0 , one sees that

$$\begin{aligned} \rho &= \frac{5}{2} c_0 \chi^{3/2} + 3h_1 r_0 \chi^2 \\ &= \frac{5}{2} c_0 \left(\frac{\mu}{1 - \tau^2 \omega^2} \right)^{3/2} v^3 + r_0 h_1 \left(\frac{\mu}{1 - \tau^2 \omega^2} \right)^2 \left(-\frac{15}{4} v B_1(v) + 3v^4 \right). \end{aligned} \quad (5.38)$$

Hence, at the droplet edge, *i.e.* at $v = 0$,

$$\rho(v = 0) = -r_0 h_1 \left(\frac{\mu}{1 - \tau^2 \omega^2} \right)^2, \quad (5.39)$$

which is regular.

The computation of the action at the saddle parallels what was done in the previous section, giving the Lagrange density

$$\mathcal{L}_{\text{S}} = -c_0 \frac{\mu^{5/2} \cos^5(\psi)}{(1 - \omega^2 \tau^2)^{5/2}} - r_0 h_1 \left(\frac{\mu}{1 - \omega^2 \tau^2} \right)^3 \left(\cos^6(\psi) + \frac{5}{2} \cos^3(\psi) B_1(v) \right) \quad (5.40)$$

and the action

$$S_{\text{S}} = -\frac{5\pi^2 c_0 \mu^4}{16\sqrt{2}\omega^3} \int_{-1/\omega}^{1/\omega} \frac{d\tau}{1 - \omega^2 \tau^2} + \frac{1984\pi\mu^{9/2} r_0 h_1}{945\sqrt{2}\omega^3} \int_{-1/\omega}^{1/\omega} \frac{d\tau}{(1 - \omega^2 \tau^2)^{3/2}}. \quad (5.41)$$

The integrals over τ diverge. To regulate them, the integration bounds are restricted to

$\pm 1/\omega \mp \epsilon$ where finally one takes the $\epsilon \rightarrow 0$ limit. The result is

$$S_{\text{eff}} = -\frac{5\pi^2 c_0 \mu^4}{16\sqrt{2}\omega^4} \log\left(\frac{2}{\epsilon\omega}\right) + \frac{1984\pi^2 \mu^{9/2} r_0 h_1}{945\omega^4} \frac{1}{(\omega\epsilon)^{1/2}} + \mathcal{O}(\epsilon^{1/2}). \quad (5.42)$$

The leading term agrees with the results of [19], given in Eq. (4.8).

Now that the action at the saddle has been computed, it should be inserted into the expression for the two-point function given in Eq. (4.7). However, the NLO correction in r_0 to the action at the saddle can be reabsorbed by a field redefinition and is therefore not physical⁶. The final result is that there is no NLO correction in r_0 to the two-point function. It is interesting that the leading effective-range corrections are also found to vanish in conformal perturbation theory in the three-body sector [4]. In Ref. [40] it was shown that when computing the three-body binding energy in an EFT of contact operators, there is a discrete scale invariance which guarantees that the first-order effective-range correction to the binding energy vanishes. Such a symmetry argument does not seem to be available in the perturbation theory considered here and in Ref. [4].

5.4. Boundary effects

In the NLO calculation of the previous section, the fact that the size of the droplet changes as the Schrödinger symmetry is deformed was neglected. Here it will be shown that the shift in the boundary leads to corrections of order $\mathcal{O}(r_0^{7/3})$, which is higher order than what is considered in this work. It is important to remark that in any case, close to the LO edge, the solution that has been found diverges and does not respect the conditions one expects to be satisfied in a perturbative expansion. For this reason one can at best estimate the parametric dependence of the neglected terms. A similar situation arises also in the case of pure Schrödinger dynamics at higher order, where the EFT requires the insertion of edge operators [7, 10]. In both cases, this near-edge dynamics leads to new terms in the effective action at the saddle point, scaling with rational powers of the expansion parameter (here $r_0\sqrt{\mu}$).

The boundary of the droplet is found by imposing $X(\tau, \psi_{\text{NLO}}) = 0$. Explicitly:

$$X(\tau, \psi_{\text{NLO}}) = \frac{\mu}{1 - \tau^2 \omega^2} \cos^2(\psi_{\text{NLO}}) + \left(\frac{\mu}{1 - \omega^2 \tau^2}\right)^{3/2} r_0 \frac{h_1}{c_0} B_1(\psi_{\text{NLO}}) = 0. \quad (5.43)$$

As noted above, for $\psi \rightarrow \pi/2$ the function B_1 diverges as

$$B_1(\psi) \underset{\psi \rightarrow \pi/2}{\sim} \frac{4}{15 \cos(\psi)}. \quad (5.44)$$

6. The diverging integral can be regularized by analytic continuation, as is done in Section E. Then, the NLO term vanishes. The coefficient in front of the log, on the other hand, is physical and appears as the residue of the pole in a ratio of gamma functions.

It follows that $\pi/2 - \psi_{\text{NLO}}$ scales like $r_0^{1/3}$:

$$\cos(\psi_{\text{NLO}}) = \left(\frac{4r_0 h_1 \sqrt{\mu}}{15c_0 \sqrt{1 - \tau^2 \omega^2}} \right)^{1/3} \Rightarrow \psi_{\text{NLO}} = \frac{\pi}{2} - \left(\frac{4r_0 h_1 \sqrt{\mu}}{15c_0 \sqrt{1 - \tau^2 \omega^2}} \right)^{1/3}. \quad (5.45)$$

From this expression one can estimate the error that is made in computing the action at the saddle when integrating over ψ up to $\psi = \pi/2$, in contrast to ψ_{NLO} :

$$\Delta S \propto \frac{\mu^4}{\omega^3} \int d\tau \frac{1}{1 - \omega^2 \tau^2} \int_{\psi_{\text{NLO}}}^{\pi/2} \sin^2(\psi) \cos(\psi) d\psi \cos^5(\psi) \propto \frac{\mu^4}{\omega^3} \int d\tau \frac{(r_0 \sqrt{\mu})^{7/3}}{(1 - \omega^2 \tau^2)^{1+7/6}}. \quad (5.46)$$

Unsurprisingly, the integral over τ is divergent. However, as will be seen in the following, after regularization, there remains a finite contribution to the action at the saddle. For the moment, observe that such a contribution scales like $r_0^{7/3}$ and is parametrically smaller than the next-to-next-to-leading order (NNLO) term that one obtains by adding a new term of order $\mathcal{O}(r_0^2)$ to the action, and that will be computed in the next section.

5.5. Continuity equation and charge conservation

The solution to the EOM has been computed in terms of the parameters r_0 , $\omega = 2/\tau_{12}$ and μ . However, while the first two parameters have well-defined physical meaning, in order to compute correlation functions at fixed charge, it is necessary to express μ as function of the inserted charge Q . To do so, consider the continuity equation

$$i \frac{\partial \rho}{\partial \tau} - \frac{\partial}{\partial x^i} \left(\frac{\partial \theta}{\partial x^i} \rho \right) = iQ (\delta(\tau + 1/\omega) - \delta(\tau - 1/\omega)) \delta(\mathbf{x}). \quad (5.47)$$

Integrating this equation over the droplet will fix the charge. However, extra care is necessary for two reasons:

1. The position of the droplet edge varies over time (the Reynolds transport theorem);
2. The current $j^i = \partial^i \theta \rho$ is not zero at the droplet edge because, while the density ρ vanishes, the term $\partial^i \theta$ diverges.

Taking these issues into account, the integral form is

$$i \frac{d}{d\tau} \int_D d^3x \rho - i \int_{\partial D} \rho \mathbf{v} \cdot d\boldsymbol{\Sigma} - \int_D d^3x \partial_i (\partial^i \theta \rho) = iQ (\delta(\tau + 1/\omega) - \delta(\tau - 1/\omega)), \quad (5.48)$$

where \mathbf{v} is the Eulerian velocity of the edge.

In the radially-symmetric problem, the equation simplifies to

$$i \frac{d}{d\tau} \int_0^{R(\tau)} r^2 dr \rho(r) - i r^2 \rho(r) \dot{R}(\tau) \Big|_{r=R(\tau)} - \int_0^{R(\tau)} r^2 dr \left(\theta''(r) \rho(r) + \theta'(r) \rho(r) + \frac{2}{r} \theta'(r) \rho'(r) \right) = i \frac{Q}{4\pi} (\delta(\tau + 1/\omega) - \delta(\tau - 1/\omega)), \quad (5.49)$$

where $R(\tau) = R_{\text{LO}}(1 - \omega^2 \tau^2)^{1/2}$ is the LO edge.⁷ Evaluating each term on the NLO solution gives

$$\frac{d}{d\tau} \int_0^{R(\tau)} r^2 dr \rho(r) = \frac{5\pi}{16\sqrt{2}} \left(\frac{\mu}{\omega} \right)^3 (\delta(\tau + 1/\omega) - \delta(\tau - 1/\omega)) - \frac{\sqrt{2}}{6} \frac{h_1 r_0 \sqrt{\omega}}{\sqrt{1 - \omega^2 \tau^2}} \left(\frac{\mu}{\omega} \right)^{7/2} \quad (5.50)$$

$$r^2 \rho(r) \dot{R}(\tau) \Big|_{r=R(\tau)} = -\frac{\sqrt{2}}{2} \frac{h_1 r_0 \sqrt{\omega}}{\sqrt{1 - \omega^2 \tau^2}} \left(\frac{\mu}{\omega} \right)^{7/2}, \quad (5.51)$$

$$\int_0^{R(\tau)} r^2 dr \left(\theta''(r) \rho(r) + \theta'(r) \rho(r) + \frac{2}{r} \theta'(r) \rho'(r) \right) = \frac{\sqrt{2}}{3} i \frac{h_1 r_0 \sqrt{\omega}}{\sqrt{1 - \omega^2 \tau^2}} \left(\frac{\mu}{\omega} \right)^{7/2}. \quad (5.52)$$

The $\mathcal{O}(r_0)$ terms cancel among each other and no time-independent $\mathcal{O}(r_0)$ term remains. The continuity equation then reduces to

$$\frac{5c_0 \pi^2}{4\sqrt{2}} \left(\frac{\mu}{\omega} \right)^3 = Q \quad (5.53)$$

or, equivalently, using the Bertsch parameter,

$$\left(\frac{\mu}{\omega} \right)^3 = 3\xi^{3/2} Q, \quad (5.54)$$

in agreement with Eq. (4.6). This fixes the value of μ as a function of Q in agreement with the result in [19], where this equation had been interpreted as charge conservation.

While this calculation has only computed the $\mathcal{O}(r_0)$ term, the same cancellation must occur at all orders. As discussed in the previous section, each power of r_0 in the expression of the density ρ is accompanied by powers of $(1 - \omega^2 \tau^2)$. All of these terms have to cancel separately on the left-hand side (LHS) of the differential form of the continuity equation because there is no such τ dependence on the right-hand side (RHS). The conclusion is that the expression of μ as function of Q is valid to all orders in r_0 .

7. For this argument it is sufficient to consider the edge at leading order. The NLO correction to the edge would reflect into higher-order corrections.

6. Second-order effective range correction

6.1. EOM in the oscillator frame

Consider now the solution of the EOM for the action

$$L = -c_0 X^{5/2} - h_1 r X^3 - h_2 r^2 X^{7/2}. \quad (6.1)$$

Following the same procedure as above, the solution at order $O(r_0^2)$ in the oscillator frame can be written as

$$\tilde{\theta}(\tilde{\tau}, \tilde{\nu}) = \tilde{\theta}_0(\tilde{\tau}, \tilde{\nu}) + \frac{\mu^{3/2}}{\omega} r_0 \tilde{\theta}_1(\tilde{\tau}, \tilde{\nu}) + \frac{\mu^2}{\omega} r_0^2 \tilde{\theta}_2(\tilde{\tau}, \tilde{\nu}). \quad (6.2)$$

The key observation is that even though the EOM is not separable, it becomes so order by order and one can decompose

$$\tilde{\theta}_2(\tilde{\tau}, \tilde{\nu}) = i \sinh(2\omega\tilde{\tau}) B_2(\tilde{\nu}), \quad (6.3)$$

where, in analogy with the first-order case, only the term that survives after minimizing the energy has been given. The second-order EOM becomes

$$\tilde{\nu}(1 - \tilde{\nu}^2) B_2''(\tilde{\nu}) + (2 - 5\tilde{\nu}^2) B_2'(\tilde{\nu}) + 12\tilde{\nu} B_2(\tilde{\nu}) = f_2(\tilde{\nu}), \quad (6.4)$$

$$f_2(\tilde{\nu}) = \frac{210c_0 h_2 \tilde{\nu}^{10} + 2h_1^2 (8 + 12\tilde{\nu}^2 + 22\tilde{\nu}^4 - 36\tilde{\nu}^6 + 9\tilde{\nu}^8 - 64\tilde{\nu}^{10})}{75c_0^2 \tilde{\nu}^5}. \quad (6.5)$$

This equation can be solved explicitly using variation of parameters since the associated homogeneous equation is hypergeometric. It admits the solution

$$C_2(\tilde{\nu}) = k_1 \frac{1 - 8\tilde{\nu}^2 + 8\tilde{\nu}^4}{\tilde{\nu} \sqrt{1 - \tilde{\nu}^2}} + k_2 (1 - 2\tilde{\nu}^2). \quad (6.6)$$

The integration constant k_1 is fixed to 0 by requiring the solution to be regular in the center of the droplet $\tilde{\nu} = 1$, so the associated solution just yields one term involving a constant k_2 that is fixed to zero by minimization of the energy. The final result is

$$\begin{aligned} B_2(\tilde{\psi}) &= B_2^2 \frac{h_2}{c_0} + B_2^1 \left(\frac{h_1}{c_0} \right)^2 = \\ &= - \frac{7}{4800 \sin(2\tilde{\psi})} \left[60\tilde{\psi} \cos(4\tilde{\psi}) + 50 \sin(2\tilde{\psi}) + 31 \sin(4\tilde{\psi}) - 6 \sin(6\tilde{\psi}) \right] \frac{h_2}{c_0} \\ &+ \left[\frac{384 \cos(4\tilde{\psi}) - 26609 \cos(2\tilde{\psi}) - 8728}{36000} + \frac{4}{15} \cos(2\tilde{\psi}) \log(\cos(\tilde{\psi})) \right] \frac{h_2}{c_0} \end{aligned}$$

$$-\frac{7\psi \cos(4\tilde{\psi})}{80 \sin(2\tilde{\psi})} + \frac{4}{75 \cos^2(\tilde{\psi})} + \frac{4}{225 \cos^4(\tilde{\psi})} \left[\left(\frac{h_1}{c_0} \right)^2 \right]. \quad (6.7)$$

The inhomogeneous solution diverges at the boundary of the droplet $v = 0$ as

$$B_2(v) \xrightarrow{v \rightarrow 0} \left(\frac{2h_1}{15c_0} \right)^2 \frac{1}{v^4} + \frac{1}{3} \left(\frac{2h_1}{5c_0} \right)^2 \frac{1}{v^2} - \frac{7\pi}{320c_0^2} \frac{h_1^2 + c_0 h_2}{v} - \frac{4}{15} \left(\frac{h_1}{c_0} \right)^2 \log v. \quad (6.8)$$

Recall that the NLO solution was understood to be valid only up to a distance $O(r_0^{2/3})$ from $v = 0$, so the singularity in $v = 0$ is not a problem.

6.2. Action at the saddle in the flat frame

Reverting to the flat frame gives:

$$\begin{aligned} X = & \frac{\mu}{1 - \omega^2 \tau^2} \cos^2(\psi) - \frac{h_1}{c_0} \left(\frac{\mu}{1 - \omega^2 \tau^2} \right)^{3/2} r_0 B_1(\psi) \\ & - \left(\frac{\mu}{1 - \omega^2 \tau^2} \right)^2 \frac{r_0^2}{4} \left[8 \frac{h_2}{c_0} (1 + \omega^2 \tau^2) B_2^{(2)}(\psi) \right. \\ & \left. + \left(\frac{h_1}{c_0} \right)^2 \left(8(1 + \omega^2 \tau^2) B_2^{(1)}(\psi) - \tau^2 \omega^2 \tan^2(\psi) B_1'(\psi)^2 \right) \right]. \quad (6.9) \end{aligned}$$

As expected, each order in r_0 comes with an extra $(1 - t^2 \omega^2)^{1/2}$ in the denominator. The Lagrange density at the saddle is

$$\mathcal{L}_{\text{saddle}} = -c_0 \left(\frac{\mu}{1 - \omega^2 \tau^2} \right)^{5/2} L_0 - r_0 \left(\frac{\mu}{1 - \omega^2 \tau^2} \right)^3 h_1 L_1 - r_0^2 \left(\frac{\mu}{1 - \omega^2 \tau^2} \right)^{7/2} \left(\frac{h_1^2}{c_0} L_2^{(1)} + h_2 L_2^{(2)} \right) \quad (6.10)$$

with

$$L_0 = \cos^5(\psi), \quad (6.11)$$

$$L_1 = \frac{5}{2} B_1(\psi) \cos^3(\psi) - \cos^6(\psi), \quad (6.12)$$

$$\begin{aligned} L_2^{(1)} = & \frac{15}{8} B_1(\psi)^2 \cos(\psi) - 5(1 + \omega^2 \tau^2) B_2^{(1)}(\psi) \cos^3(\psi) - 3B_1(\psi) \cos^4(\psi) \\ & + \frac{5}{8} \tau^2 \omega^2 B_1'(\psi)^2 \cos(\psi) \sin^2(\psi), \quad (6.13) \end{aligned}$$

$$L_2^{(2)} = \cos^7(\psi) - 5(1 + \omega^2 \tau^2) B_2^{(2)}(\psi) \cos^3(\psi). \quad (6.14)$$

Now one proceeds as before to the action at the saddle point.⁸ The $\mathcal{O}(r_0^2)$ term comprises four corrections:

$$S_{\text{eff}}|_{r_0^2} = r_0^2 \frac{\mu^5}{\omega^3} \int_{-1/\omega}^{1/\omega} d\tau \frac{h_1^2/c_0 (s_{2,1} + s_{2,2}\omega^2\tau^2) + h_2 (s_{2,3} + s_{2,4}\omega^2\tau^2)}{(1 - \omega^2\tau^2)^2} \quad (6.15)$$

with

$$s_{2,1} = \frac{13787\pi^2}{12800\sqrt{2}} + \frac{\pi^2 \log(2)}{6\sqrt{2}}, \quad s_{2,2} = \frac{48281\pi^2}{38400\sqrt{2}} + \frac{\pi^2 \log(2)}{6\sqrt{2}}, \quad s_{2,3} = -\frac{273\pi^2}{2500\sqrt{2}}, \quad s_{2,4} = -\frac{833\pi^2}{2560\sqrt{2}}. \quad (6.16)$$

Regularizing the integral over τ , one again finds a term that diverges as $1/\epsilon$ and can be reabsorbed in the definition of the operators, and a logarithmic divergence, whose coefficient is the physical quantity of interest:

$$\begin{aligned} S_{\text{eff}}|_{r_0^2} &= \frac{r_0^2 \mu^5}{2\omega^4} \left((s_{2,1} - s_{2,2}) \frac{h_1^2}{c_0} + (s_{2,3} - s_{2,4}) h_2 \right) \log\left(\frac{2}{\omega\epsilon}\right) \\ &= \frac{r_0^2 \mu^5}{\omega^4} \left(-\frac{173\pi^2}{1920\sqrt{2}} \frac{h_1^2}{c_0} + \frac{7\pi^2}{64\sqrt{2}} h_2 \right) \log\left(\frac{2}{\omega\epsilon}\right). \end{aligned} \quad (6.17)$$

This is the final result for the correction of order $\mathcal{O}(r_0^2)$ to the effective action and to the two-point function. As expected, the numerical coefficients are of order one.

$$-\frac{173\pi^2}{1920\sqrt{2}} \approx -0.629, \quad \frac{7\pi^2}{64\sqrt{2}} \approx 0.763. \quad (6.18)$$

7. Regularization of the two-point function

This section considers the regularization of the two-point function at the temporal boundary in some detail. The two-point function at $\mathcal{O}(r_0^2)$ is

$$G_Q(-1/\omega, 1/\omega) = \mathcal{O}_{\Delta,Q}(-1/\omega) \mathcal{O}_{\Delta,-Q}(1/\omega) e^{-S_{\text{eff}}}. \quad (7.1)$$

Each of the three factors on the right-hand side of this equation are divergent. The mutual cancellation of the divergences will give the final result. The operator $\mathcal{O}_{\Delta,Q}$ is expressed in terms of θ by identifying its charge and operator dimension and is given by Eq. (4.1). As all divergences should be accounted for, it is convenient to rewrite the correlation function in the form of an integral over τ , expressing the insertions at the

8. The integration bounds for ψ are again 0 and $\pi/2$, up to higher-order corrections.

boundary as integrals of total derivatives:

$$\mathcal{O}_{\Delta,Q}(-1/\omega)\mathcal{O}_{\Delta,-Q}(1/\omega) = \mathcal{N}^2(\mathcal{X}(-1/\omega)\mathcal{X}(1/\omega))^{\Delta/2}e^{iQ(\theta(1/\omega)-\theta(-1/\omega))} \quad (7.2)$$

$$= \mathcal{N}^2\mathcal{X}(0)^\Delta \exp\left(\int_{-1/\omega}^{1/\omega} d\tau \frac{\Delta}{2}|\partial_\tau \log \mathcal{X}(\tau)| + iQ \partial_\tau \theta(\tau)\right). \quad (7.3)$$

Above it was found that at NNLO,

$$S_{\text{reg}} = Q^{4/3}\omega \int_{-1/\omega}^{1/\omega} d\tau \left(s_0 \frac{1}{1-\omega^2\tau^2} + h_1 s_1 \kappa \frac{1}{(1-\omega^2\tau^2)^{3/2}} + \frac{\kappa^2}{(1-\omega^2\tau^2)^2} \left(\frac{h_1}{c_0} (s_{2,1} + s_{2,2}\omega^2\tau^2) + h_2 (s_{2,3} + s_{2,4}\omega^2\tau^2) \right) \right), \quad (7.4)$$

$$\partial_\tau \theta = i\gamma \frac{\omega}{1-\omega^2\tau^2} + i \frac{h_1}{c_0} \gamma \omega \frac{B_1(1)\kappa}{(1-\omega^2\tau^2)^{3/2}} + \frac{2i\gamma\omega(1-\omega^2\tau^2)B_2(1)\kappa^2}{(1-\omega^2\tau^2)^2} \quad (7.5)$$

$$\partial_\tau \log \mathcal{X} = \frac{2\tau\omega}{1-\omega^2\tau^2} - \frac{h_1}{c_0} \gamma \omega^2 \frac{\tau B_1(1)\kappa}{(1-\omega^2\tau^2)^{3/2}} + \dots, \quad (7.6)$$

with $s_0 = 5\pi^2\sqrt{2}c_0/32$, $s_1 = 1984\pi\sqrt{2}/1890$ and the $s_{2,i}$ as defined in Eq. (6.16). Observe that at each order the three terms have the same analytic structure in terms of poles and branch cuts at the extrema of integration $\tau = \pm 1/\omega$.

All the integrals are divergent and require regularization. One possibility is to change the boundaries of integration,

$$\int_{-1}^1 dz \frac{1}{(1-z^2)^n} = \lim_{\epsilon \rightarrow 0} \int_{-1+\epsilon}^{1-\epsilon} dz \frac{1}{(1-z^2)^n}. \quad (7.7)$$

Another possibility is to analytically continue the power appearing in the denominator:

$$\int_{-1}^1 dz \frac{1}{(1-z^2)^n} = \lim_{\delta \rightarrow 0} \int_{-1}^1 dz \frac{1}{(1-z^2)^{n+\delta}}. \quad (7.8)$$

The two regularizations are discussed in detail for these integrals and a generalization in Appendix E.

Leading order. Using the two regularization schemes, the leading-order result is

$$\begin{aligned} \int_{-1}^1 dz \frac{s_0 Q^{4/3} - \gamma Q + \Delta |z|}{(1-z^2)} &= \lim_{\epsilon \rightarrow 0} (-\Delta + Q\gamma - s_0 Q^{4/3}) \log \epsilon - (-\Delta + Q\gamma - s_0 Q^{4/3}) \log 2 \\ &= \lim_{\delta \rightarrow 0} \frac{-\Delta + Q\gamma - s_0 Q^{4/3}}{\delta} + (\gamma Q - s_0 Q^{4/3}) \log 2. \end{aligned} \quad (7.9)$$

In both cases, the result is divergent unless

$$-\Delta + Q\gamma - s_0 Q^{4/3} = 0. \quad (7.10)$$

This is, as already observed in [19], the Legendre transform relating Δ to s_0 . The final result is

$$G_Q(-1/\omega, 1/\omega) \propto \frac{(2\gamma)^\Delta}{\tau_{12}^\Delta}, \quad (7.11)$$

as predicted by Schrödinger invariance.

Next-to-leading order. At NLO, in the δ regularization, the three contributions vanish separately since for the S and θ part,

$$\lim_{\delta \rightarrow 0} \int_{-1}^1 dz \frac{1}{(1-z^2)^{3/2}} = \lim_{\delta \rightarrow 0} \sqrt{\pi} \frac{\Gamma(-1/2 - \delta)}{\Gamma(-\delta)} = 0. \quad (7.12)$$

In the ϵ regularization, there remains a divergent contribution

$$\lim_{\epsilon \rightarrow 0} \int_{-1+\epsilon}^{1-\epsilon} dz \frac{1}{(1-z^2)^{3/2}} = \lim_{\epsilon \rightarrow 0} \sqrt{\frac{2}{\epsilon}}. \quad (7.13)$$

This term is however constant in the sense that it does not depend on $1/\tau_{12} = \omega$ and can be absorbed in the normalization of the operators in the two-point function.

As for the contribution from the integral of $|\partial_\tau \log X|$, this cancels with $\exp(\Delta X_{\text{NLO}}(0))$. The regularization of the integral gives

$$\lim_{\delta \rightarrow 0} \int_{-1}^1 dz \frac{|z|}{(1-z^2)^{3/2+\delta}} = \lim_{\delta \rightarrow 0} \frac{1}{-1/2 - \delta} = -2, \quad (7.14)$$

and so the contribution to the two-point function is

$$X(0)_{\text{NLO}}^{\Delta} \exp \left[\frac{\Delta}{2} \int_{-1/\tau}^{1/\tau} d\tau |\partial_{\tau} \log(X)_{\text{NLO}}| \right] = \exp \left[-\Delta \frac{h_1}{c_0} \gamma_{\kappa} B_1(1) \right] \exp \left[\lim_{\delta \rightarrow 0} \left(-\frac{\Delta h_1}{2c_0} \gamma_{\kappa} B_1(1) \int_{-1}^1 dz \frac{1}{(1-z^2)^{3/2-\delta}} \right) \right] = 1. \quad (7.15)$$

The result is then that *the NLO correction in r_0 is identically zero.*

Next-to-next-to-leading order. Using the same argument as above, one finds that the X^{Δ} contribution vanishes identically at NNLO. It is convenient to collect the remaining NNLO terms in the form:

$$\left(-2\gamma_{\kappa} Q B_2(1) + \left(\frac{h_1}{c_0} s_{2,2} + h_2 s_{2,4} \right) \right) \int_{-1}^1 dz \frac{1+z^2}{(1-z^2)^2} + \left(\frac{h_1}{c_0} (s_{2,1} - s_{2,2}) + h_2 (s_{2,3} - s_{2,4}) \right) \int_{-1}^1 dz \frac{1}{(1-z^2)^2}. \quad (7.16)$$

Both integrals need to be regularized, and one finds, respectively,

$$\int_{-1}^1 dz \frac{1+z^2}{(1-z^2)^2} = \lim_{\delta \rightarrow 0} \frac{\sqrt{\pi} \Gamma(-\delta-1)}{\Gamma(-1/2-\delta)} = -1 = \lim_{\epsilon \rightarrow 0} \left(\frac{1}{\epsilon} \right) - \frac{1}{2} \quad (7.17)$$

and

$$\int_{-1}^1 dz \frac{1}{(1-z^2)^2} = \lim_{\delta \rightarrow 0} \left(-\frac{1}{2\delta} \right) - \frac{1}{2} + \log(2) = \lim_{\epsilon \rightarrow 0} \left(\frac{1}{2\epsilon} - \frac{1}{2} \log(\epsilon) \right) + \frac{1}{2} \log(2) - \frac{1}{4}. \quad (7.18)$$

The $1/\delta$ and $\log(\epsilon)$ divergences come again with the same coefficient. Their cancellation results in the $O(\kappa^2)$ correction to the Legendre transform in Eq. (7.10):

$$\Delta = Q\gamma - s_0 Q^{4/3} - \frac{\kappa^2 Q^{4/3}}{2} \left(\frac{h_1^2}{c_0} (s_{2,1} - s_{2,2}) + h_2 (s_{2,3} - s_{2,4}) \right). \quad (7.19)$$

The coefficient in front of the integrals does not depend on $\omega = 2/\tau_{12}$, and all the other (scheme-dependent) terms can be treated as constants to be absorbed in the normalization of the operators. Note that the NNLO corrections to the insertions do not influence the form or the value of the two-point function.

The final result is once more

$$G_Q(-1/\omega, 1/\omega) \propto \frac{1}{\tau_{12}^\Delta}, \quad (7.20)$$

as expected.

8. Leading-order solution for the scattering length corrections

The same technique that was used to analyze the effective-range corrections can be used to study the effect of the breaking of Schrödinger invariance due to a finite scattering length⁹. In this case, the Lagrange density is

$$\mathcal{L} = -c_0 X^{5/2} - g_1 a^{-1} X^2 + \mathcal{O}(a^{-2}). \quad (8.1)$$

In the oscillator frame,

$$\tilde{\mathcal{L}} = -c_0 \tilde{X}^{5/2} - \frac{g_1}{a \cosh(\omega \tilde{\tau})} \tilde{X}^2. \quad (8.2)$$

One can search for isotropic solutions of the form

$$\tilde{\theta}(\tilde{\tau}, \tilde{\nu}) = -i\mu\tilde{\tau} + i\frac{\mu^{1/2}}{\omega} \frac{g_1}{a} \tilde{\theta}_1(\tilde{\tau}, \tilde{\nu}). \quad (8.3)$$

The NLO EOM is then found to be

$$3\tilde{\nu} \frac{\partial^2}{\partial \tilde{\tau}^2} \tilde{\theta}_1 + \omega^2 \tilde{\nu} (1 - \tilde{\nu}^2) \tilde{\theta}_1'' + (2 - 5\tilde{\nu}^2) \omega^2 \tilde{\theta}_1' = -\frac{8}{5c_0} \tilde{\nu}^2 \omega \frac{d}{d\tilde{\tau}} \frac{1}{\cosh(\omega \tilde{\tau})}, \quad (8.4)$$

which is the same as Eq. (5.18), but with a different rhs. This equation is inhomogeneous and does not admit a solution by simple separation of variables. Consider, however, the

9. These effects were studied in Ref. [19]. Here it is shown that the results obtained in that paper are valid in the presence of boundary terms.

n	0	1	2	3
$\varphi_{1,n}$	$-4/15$	0	0	$-2/4725$
$\varphi_{2,n}$	$4/15$	0	$2/75$	$-26/945$

Table 1 – First coefficients in the expansions of $\phi_{1,2}$

ansatz

$$\tilde{\theta}_1(\tilde{\tau}, \tilde{\nu}) = \frac{1}{\tilde{\nu}} \phi_1(\tilde{\tau}) + \tilde{\nu} \phi_2(\tilde{\nu}), \quad (8.5)$$

which reduces the EOM to a system of ODES for ϕ_1 and ϕ_2 :

$$\begin{cases} \ddot{\phi}_1(\tau) + \omega^2 \phi_1(\tau) + \frac{2}{3} \omega^2 \phi_2(\tau) = 0, \\ \ddot{\phi}_2(\tau) - \frac{5}{3} \omega^2 \phi_2(\tau) + \frac{8\omega^2}{15c_0} \frac{\sinh(\omega\tau)}{\cosh^2(\omega\tau)} = 0. \end{cases} \quad (8.6)$$

The associated homogeneous system is hypergeometric and can be solved explicitly, and once again variation of parameters may be used to obtain

$$\begin{aligned} \phi_1(\tilde{\tau}) = \frac{2}{5c_0(3 + \sqrt{15})} e^{\omega\tilde{\tau}} & \left((4 + \sqrt{15}) {}_2F_1 \left(1, \frac{3-\sqrt{15}}{6} \middle| \frac{9-\sqrt{15}}{6} \right. \middle| -e^{-2\omega\tilde{\tau}} \right) - {}_2F_1 \left(1, \frac{3+\sqrt{15}}{6} \middle| \frac{9+\sqrt{15}}{6} \right. \middle| -e^{-2\omega\tilde{\tau}} \right) \\ & + \frac{\sqrt{2}}{15c_0} e^{i\pi/4} e^{\omega\tilde{\tau}} {}_2F_1 \left(\frac{1-i}{2}, 1 \middle| \frac{3-i}{2} \right. \middle| -e^{-2\omega\tilde{\tau}} \right) + \text{c.c.}, \end{aligned} \quad (8.7)$$

$$\phi_2(\tilde{\tau}) = -\frac{4}{15c_0} e^{\omega\tilde{\tau}} \left((3 + \sqrt{15}) {}_2F_1 \left(1, \frac{3-\sqrt{15}}{6} \middle| \frac{9-\sqrt{15}}{6} \right. \middle| -e^{2\omega\tilde{\tau}} \right) + (3 - \sqrt{15}) {}_2F_1 \left(1, \frac{3+\sqrt{15}}{6} \middle| \frac{9+\sqrt{15}}{6} \right. \middle| -e^{2\omega\tilde{\tau}} \right). \quad (8.8)$$

These explicit expressions are exact but complicated to use. A useful observation is that ϕ_1 and ϕ_2 admit an expansion in hyperbolic sines of odd multiples of $\omega\tilde{\tau}$:

$$\phi_1 = \frac{1}{c_0} \sum_{n=0}^{\infty} \varphi_{1,n} \sinh((2n+1)\omega\tau), \quad \phi_2 = \frac{1}{c_0} \sum_{n=0}^{\infty} \varphi_{2,n} \sinh((2n+1)\omega\tau). \quad (8.9)$$

The first few coefficients are given in Table 1. With this observation, one reverts to the flat frame in which each $\sinh((2n+1)\omega\tilde{\tau})$ turns into an odd power of $(1 - \omega^2\tau^2)$ as in Eq. (E.7). Following the same construction as in Appendix E, one concludes that all of these terms do not contribute to the action at the saddle, in analogy to all the $\mathcal{O}(r_0)$ corrections of odd order. The final result is that the only correction at $\mathcal{O}(1/a)$ is due to the evaluation of the NLO action on the LO solution in agreement with the result in [19]:

$$S_{\text{eff}}|_{\alpha^{-1}} = \frac{64 \times 3^{1/6} \sqrt{2} \pi^2 \xi^{7/4} g_1}{35 a \omega^{1/2}} Q^{7/2}. \quad (8.10)$$

9. Minkowski-space correlation functions

9.1. General procedure

In order to make contact with phenomena, the position-space correlation functions should be continued from Euclidean space back to Minkowski space, with the choice of source points $x_1 = (t, \mathbf{x})$, $x_2 = (0, \mathbf{0})$, and then, the resulting correlation function, $G_Q(x_1; x_2)$ should be Fourier transformed to obtain the momentum-space correlation function $G_Q(E, \mathbf{p})$, which is then relevant to the propagation of matter in spacetime [1, 3], as will be seen below.

9.2. Relevant deformations: the scattering length

On general grounds, one expects that the leading scattering length effects will take the form

$$\text{Im } G_Q(E, \mathbf{0}) = C_0 E^{\Delta_Q - 5/2} \left[1 + \frac{C_Q}{a\sqrt{ME}} \right], \quad (9.1)$$

where C_0 is a normalization constant that can be absorbed into the definition of the X field. In compact form, the symmetry-breaking action at the saddle point, Eq. (8.10), in Euclidean space is

$$S_{\text{SB}}|_{a^{-1}} = \frac{64\pi^2 g_1 \gamma^{7/2}}{105} a^{-1} \tau_{12}^{1/2}. \quad (9.2)$$

As this contribution is independent of the regulator ϵ , it can be directly substituted into Eq. (4.12), which is then expanded to leading order in a^{-1} . Following the procedure described above (using the Fourier transform given in Appendix B) and matching to Eq. (9.1), one finds [19]

$$C_Q(Q) = -\frac{64\pi^2 g_1 \gamma^{7/2}}{105} \frac{\Gamma(\frac{6}{2} - \Delta_Q)}{\Gamma(\frac{5}{2} - \Delta_Q)} \tan \pi \Delta_Q. \quad (9.3)$$

It is noteworthy and promising that for $Q \sim 3$ these $O(a^{-1})$ corrections in the large-charge EFT are consistent with the range of values found in Ref. [4] working directly with the three-body wavefunctions. To get a sense of the validity of perturbation theory it is convenient to define the function

$$\text{Im } \bar{G}_Q(E, \mathbf{0}) \equiv \text{Im } G_Q(E, \mathbf{0}) / \text{Im } G_Q^{\text{CFT}}(E, \mathbf{0}), \quad (9.4)$$

where the CFT superscript indicates the correlation function evaluated with $C_Q(Q) = 0$. This function is plotted in Fig. 4 vs $a\sqrt{ME}$ to illustrate the validity of the perturbative

expansion. Clearly perturbation theory works best at large scattering length and/or large energies. Note that the growth of $C_Q(Q)$ with Q suggests that for fixed, large scattering length, as Q is increased one must consider higher-energy propagation to remain in the perturbative regime.

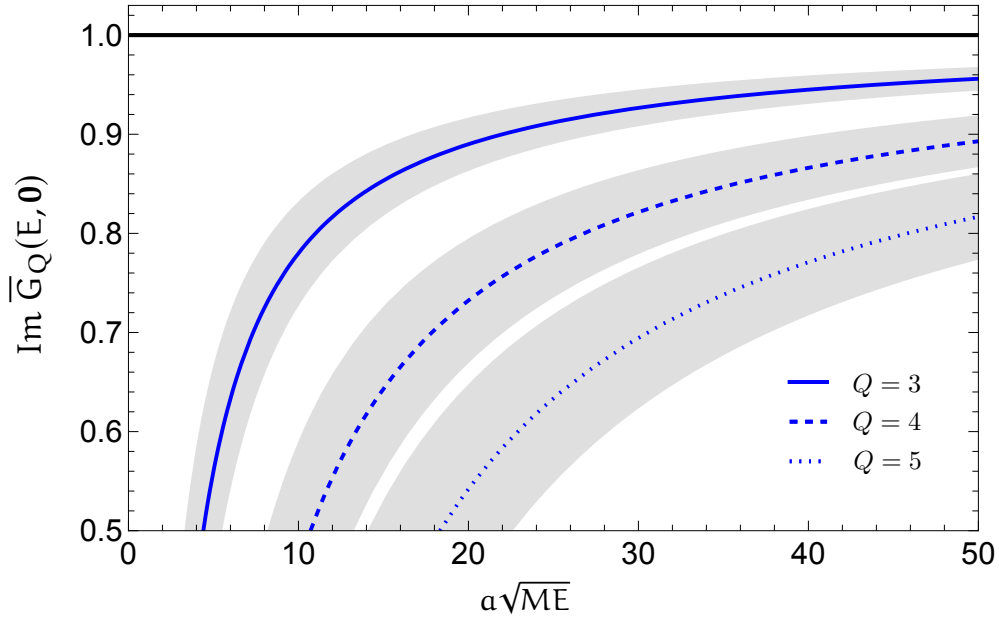


Figure 4 – Plot of the function $\text{Im } \bar{G}_Q(E, \mathbf{0})$ vs $\alpha\sqrt{ME}$ (α is assumed –without loss of generality– to be negative). The solid, dashed, dotted blue curves correspond respectively to $Q = 3, 4, 5$. The gray bands correspond to propagation of uncertainties in g_1 .

9.3. Irrelevant deformations: effective range

Here again on general grounds, one expects

$$\text{Im } G_Q(E, \mathbf{0}) = C_0 E^{\Delta_Q - 5/2} \left[1 + C'_Q r_0 \sqrt{ME} \right]. \quad (9.5)$$

However, as shown above, the leading effective-range corrections vanish and therefore

$$C'_Q = 0. \quad (9.6)$$

Note that this parallels what occurs at $Q = 3$ in Ref. [4]. (One easily sees that perturbations at all odd powers of the range are power divergent with no finite part.)

Hence, the subleading effective-range corrections should enter as

$$\text{Im } G_Q(E, \mathbf{0}) = C_0 E^{\Delta_Q - 5/2} \left[1 + C''_Q r_0^2 ME \right]. \quad (9.7)$$

In compact form, the symmetry-breaking action at the saddle point, Eq. (9.8), in Euclidean space is

$$S_{\text{SB}}|_{r_0^2} = r_0^2 \gamma^5 \left(-\frac{173\sqrt{2}\pi^2}{1920} \frac{h_1^2}{c_0} + \frac{7\sqrt{2}\pi^2}{64} h_2 \right) \tau_{12}^{-1} \log \left(\frac{\tau_{12}}{\epsilon} \right). \quad (9.8)$$

It is convenient to define

$$\alpha \equiv \gamma^5 \left(-\frac{173\sqrt{2}\pi^2}{1920} \frac{h_1^2}{c_0} + \frac{7\sqrt{2}\pi^2}{64} h_2 \right), \quad (9.9)$$

where the values of $h_{1,2}$ and c_0 extracted from lattice mc data were given in Eq. (3.14). Then, following the procedure outlined above, the conformal dimension in the presence of the symmetry breaking is

$$\Delta = \Delta_Q + r_0^2 \alpha \tau_{12}^{-1}. \quad (9.10)$$

It is not particularly surprising that the conformal dimension is spacetime dependent in the absence of Schrödinger symmetry. This then leads to the solution

$$G(x_1, x_2) = G_{\text{CFT}}(x_1, x_2) \tau_{12}^{-r_0^2 \alpha \tau_{12}^{-1}}. \quad (9.11)$$

To leading order in α and keeping terms of order $\mathcal{O}(\tau_{12}^{-1} \log \tau_{12})$,

$$G(x_1, x_2) = G_{\text{CFT}}(x_1, x_2) \left[1 - r_0^2 \alpha \tau_{12}^{-1} \log(\tau_{12} \lambda) \right], \quad (9.12)$$

where λ is an arbitrary energy scale. As the sole momentum scale is r_0^{-1} , one expects $\lambda^{-1} \propto M r_0^2$. The constant of proportionality will be chosen below to optimize perturbation theory.

Now, continuing back to Minkowski space, choosing the source points $x_1 = (t, \mathbf{x})$, $x_2 = (0, \mathbf{0})$, and using the Fourier transform found in Appendix B gives

$$C_Q''(Q, E) = \gamma^5 \left(-\frac{173\sqrt{2}\pi^2}{1920} \frac{h_1^2}{c_0} + \frac{7\sqrt{2}\pi^2}{64} h_2 \right) \frac{\Gamma\left(\frac{3}{2} - \Delta_Q\right)}{\Gamma\left(\frac{5}{2} - \Delta_Q\right)} \times \left[\psi\left(\frac{3}{2} - \Delta_Q\right) + \pi \tan \pi \Delta_Q - \log(E \lambda^{-1}) \right]. \quad (9.13)$$

Note that

$$\psi\left(\frac{3}{2} - \Delta_Q\right) \xrightarrow{\Delta_Q \rightarrow \infty} -\frac{1}{\Delta_Q} + \mathcal{O}(\Delta_Q^{-2}) - \pi \tan \pi \Delta_Q + \log(\Delta_Q). \quad (9.14)$$

Therefore, asymptotically, the harmonic contribution cancels, as is also the case with the scattering length corrections in Eq. (9.3) [19]. The large logarithm can be removed by now choosing $\lambda^{-1} = \Delta_Q M r_0^2$. Plotting $\text{Im } \bar{G}_Q(E, \mathbf{0})$ vs $r_0 \sqrt{ME}$ in Fig. 5 indicates the validity of the perturbative expansion. One sees that there is very little variation between $Q = 3$ and $Q = 6$. Because effective-range effects enter as an irrelevant deformation, perturbation theory works best for small effective ranges and/or small energies. Note that the function C_Q'' varies more slowly with Q than C_Q (asymptotically as $Q^{1/3}$ as compared to $Q^{11/6}$).

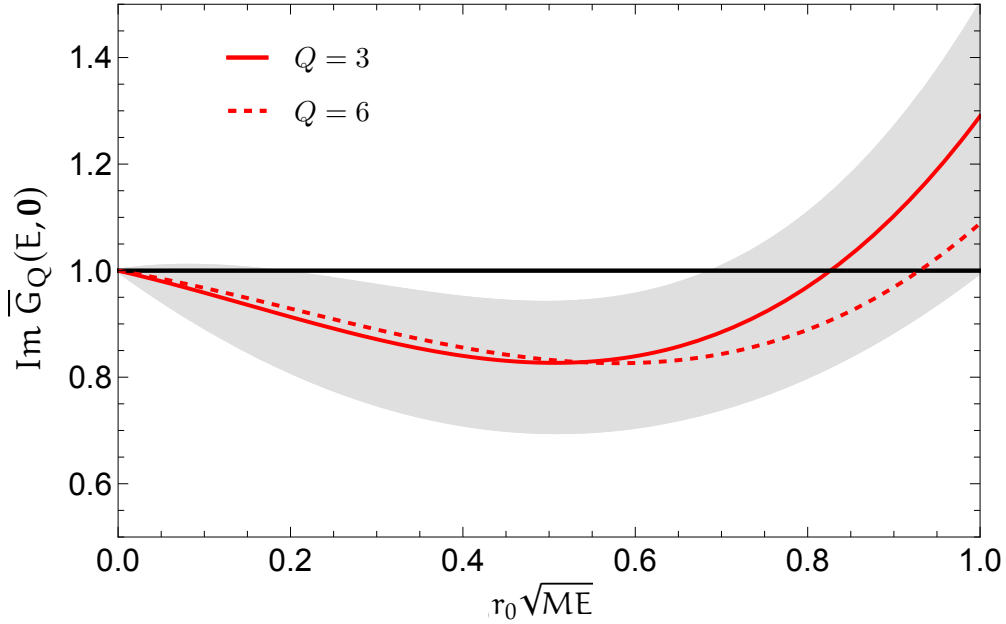


Figure 5 – Plot of the function $\text{Im } \bar{G}_Q(E, \mathbf{0})$ vs $r_0 \sqrt{ME}$. The solid and dashed red curves corresponds to $Q = 3$ and $Q = 6$. The gray bands correspond to propagation of uncertainties in $h_{1,2}$.

10. Unnuclear matter

10.1. EFT of neutron matter

To this point, the EFT of fermions near unitarity has been treated as generic. In this section, the focus will be on the specific case of neutron matter. Following Ref. [41], the values of the (unmeasured) neutron-neutron effective-range parameters are estimated to be $a = -18.5$ fm and $r_0 = 2.7$ fm. The neutrons have mass $M = 939$ MeV and the lightest DOF that is integrated out of the EFT is the pion with mass $M_\pi = 140$ MeV, whose t-channel exchange in the neutron-neutron scattering amplitude gives rise to a branch-point singularity in the complex k -plane at $M_\pi/2$. Hence $r_0^{-1} \sim M_\pi/2$ formally

sets the high-momentum scale in EFT($\not\lambda$), the EFT of contact operators which describes the interactions of neutrons and protons at very low momentum transfers where the pion is integrated out of the EFT. The branch-point singularity due to t-channel pion exchange is in practice weak and therefore in most applications EFT($\not\lambda$) extends to M_π . While in EFT($\not\lambda$) the low scale is at zero, the threshold for scattering, in the large-charge EFT the low scale is set by a^{-1} as the EFT is an expansion about the unitary fixed point. As one probes momenta k such that $ka < 1$ then a different EFT is required, which is an expansion about the non-interacting fixed point. Therefore, the large-charge EFT of neutron matter is formally valid for momenta in the range $a^{-1} < k, k_F < r_0^{-1}$, and in practice may be valid in the range $a^{-1} < k, k_F < M_\pi$. Translating to energy scales, this corresponds to energies between 0.1 and 6 MeV and 0.1 and 21 MeV, respectively. The hierarchy of scales is illustrated in Fig. 6.

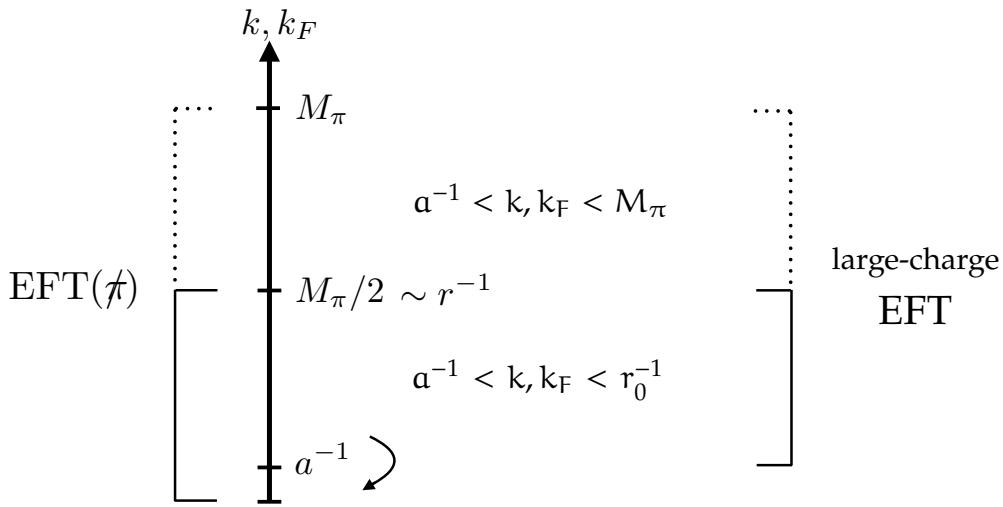


Figure 6 – Hierarchy of scales of EFT($\not\lambda$). The dotted regions denote the “effective” region of validity of the EFT. The arrow denotes a transition from the large-charge EFT, which is defined about the nontrivial unitary fixed point, to an EFT description about the trivial, non-interacting, fixed point.

10.2. Deformation and perturbative window

In neutron matter, both kinds of deformation should be considered and therefore,

$$\text{Im } G(E, \mathbf{0}) = C_0 E^{\Delta_Q - 5/2} \left[1 + C_Q \left(a \sqrt{ME} \right)^{-1} + C_Q'' r_0^2 ME \right]. \quad (10.1)$$

Fig. 7 is a plot of $\text{Im } \bar{G}_Q(E, \mathbf{0})$ vs E (MeV) for $Q = 3, 4, 5, 6$. Note that the substantial uncertainties in the coupling constants have not been propagated in this plot for clarity of presentation. Perhaps the most interesting observation is that the scattering-length and

effective-range deformations enter with opposite signs and there is therefore a partial cancellation which implies that for each Q , there is an energy at which the Schrödinger symmetry is restored. One sees that the energy window in which perturbation theory is valid is rather narrow for each Q value. However, as discussed in the introduction, for instance at SAMURAI, there is excellent energy resolution of the final-state neutrons which in principle allows one to focus on the regions of enhanced symmetry. The fundamental obstacle from the theory side is the large uncertainties in the coupling constants, particularly h_2 . However, it may be possible to improve these determinations using quantum mc simulations of the energy density.

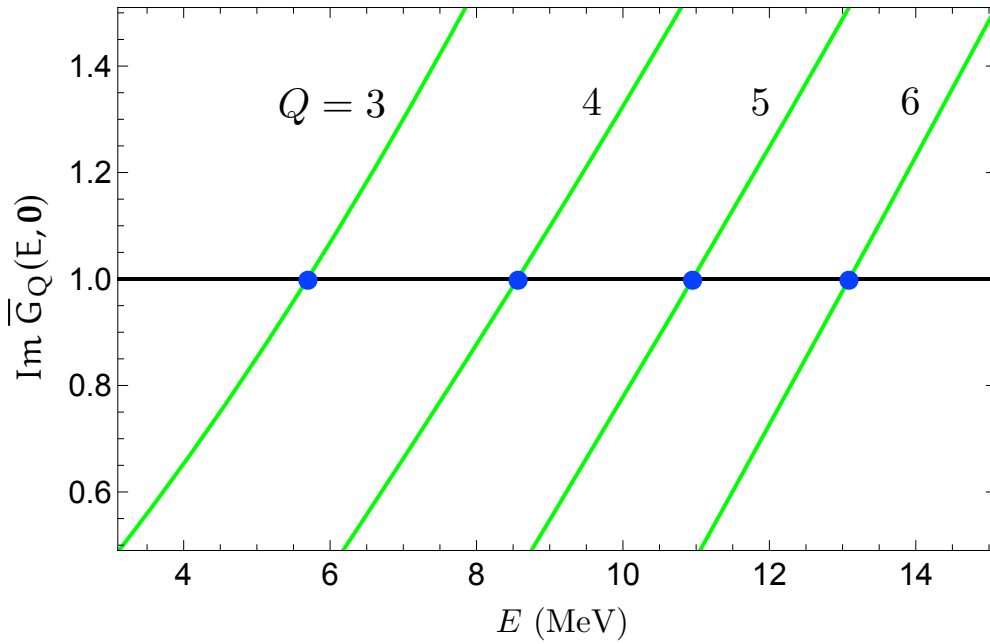


Figure 7 – Plot of the function $\text{Im } \bar{G}_Q(E, \mathbf{0})$ vs E (MeV). The green curves corresponds to $Q = 3, 4, 5, 6$. The blue dots denote the kinematical points at which the deformations cancel.

10.3. Three-body example

Following Ref. [1], consider the process

$$\pi^- + {}^3\text{H} \rightarrow \gamma + \text{nnn}, \quad (10.2)$$

which has been studied in Ref. [42], and whose theoretical predictions of the capture rate, using the AV18 two-nucleon potential and the Urbana IX three-body force, can be treated as “data” for the comparison with the predictions from the large-charge EFT with perturbative Schrödinger-symmetry breaking from scattering-length and effective-range

effects. The formula, Eq. (1.1) is used to obtain the capture rate, which is shown in Fig. 8. The dashed black curve follows from considering the case of free neutrons, whose conformal dimension is that of the three-body primary operator with fields assigned naive dimensions, giving $11/2$. The black curve is the unitary fixed point with the conformal dimension given by its well-known value for $Q = 3$: 4.27272 (p-wave) [4]¹⁰. As noted in Ref. [1], the proximity of this curve to the data is indicative of unnuclear behavior of the three-neutron final state. While the effective-range corrections, given by the red curve, appear controlled and perturbative, the scattering length corrections, given by the blue curve, and the combined effect, given by the green curve, appear to destroy this agreement. (Note that in all cases the gray bands arise from the uncertainties in the Lagrange-density parameters.) However, note from Fig. 7, that the perturbative window is not approached for $Q = 3$ until $E \sim 3$ MeV, and indeed the green curve in Fig. 8 does cross the solid black line at around $E \sim 6$ MeV, indicating a perturbative window. Therefore the energies probed by this data are too low to offer a meaningful test of the perturbative expansion. (Note as well that at very low energies the blue curve is negative, in violation of unitarity.) Presumably the perturbative window can be extended to lower energies by considering $\mathcal{O}(1/a^2)$ corrections. A more ambitious proposal would be to sum $1/a$ corrections to all orders in the two-point function of the large-charge operator about the unitarity fixed point. This would give an expression for the two-point function along the entire RG trajectory connecting the interacting and non-interacting fixed points [4].

11. Conclusion

With few exceptions, quantum field theories of nature tend to be far from conformal fixed points, and in most exceptions that are relevant to experiment, require lattice field theory simulations in order to extract physical observables. An interesting system in this regard in the non-relativistic domain is the unitary Fermi gas, which is described by a NRCFT. This system is superfluid and remains superfluid in the presence of small deformations away from the Schrödinger symmetry limit. In the symmetry limit the superfluid EFT has subsectors of fixed charge which admit a large-charge expansion. This allows the exact closed-form determination of correlation functions which encode the propagation of conformal superfluid matter in space and time. In the nuclear physics context, where, for instance, the unitary fermions are taken to be neutrons, this conformal superfluid matter has been dubbed unnuclear matter [1], as it does not have a particle interpretation. Nuclear reactions with few-body systems of neutrons in the final state offer a concrete experimental realization of unnuclear matter. Of course, describing a

10. Note that while the large-charge value of the conformal dimension at $Q = 3$, taken from Eq. (4.10), is only about one half this value, subleading corrections in the Schrödinger limit, which involve new undetermined constants [7], can be chosen to reproduce the $Q = 3$ value exactly. This is done in Appendix A.

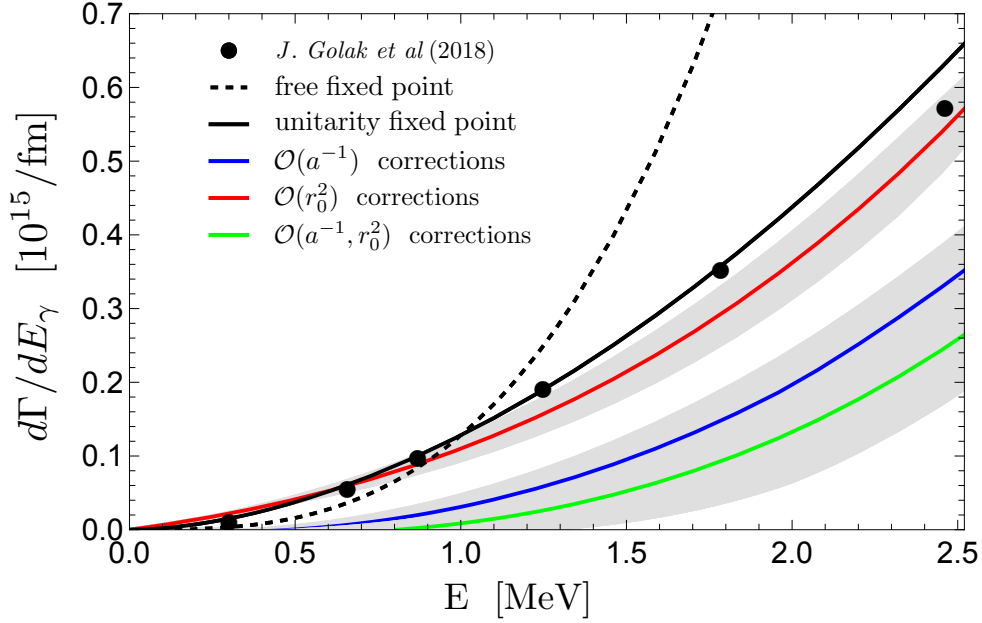


Figure 8 – Energy (center-of-mass) spectrum of three neutrons in the reaction ${}^3\text{H}(\pi^-, \gamma){}^3\text{n}$. The black circles give the calculations by Golak et al. in Ref. [42]. The various curves and regions are explained in the main text.

few-body system of neutrons as an expansion whose leading order is a NRCFT requires a quantitative measure of the symmetry breaking due to scattering length, effective range and other shape parameter effects which are clearly present in the two-neutron system and explicitly break the Schrödinger symmetry. This has been done here. The main conclusions of this study are:

- Schrödinger-symmetry breaking corrections to the large-charge two-point function have been computed in perturbation theory around the large-charge ground state. Closed-form expressions have been found for the Goldstone field perturbation by making use of a coordinate transformation to the oscillator frame, which decouples the temporal dependence.
- The Schrödinger-symmetry breaking corrections are determined by a priori unknown Lagrange-density parameters. These parameters contribute to the energy density of the superfluid matter, and have been computed using quantum MC simulations. The predictive power of the large-charge EFT relies on the accuracy with which these parameters are determined.
- The $\mathcal{O}(r_0)$ effective-range effects have been found to vanish in the large-charge EFT, as was found for the three-body case in Ref. [4]. The $\mathcal{O}(r_0^2)$ effective-range effects have been calculated, and together with the $\mathcal{O}(a^{-1})$ scattering-length effects calculated in Ref. [19], provide the leading Schrödinger-symmetry breaking corrections to the

large-charge two-point function. Critically, the two kinds of deformation enter with opposite signs and therefore there is a partial cancellation.

- At fixed charge Q , the energy-dependent Schrödinger-symmetry breaking corrections to the large-charge two-point function are found to be perturbative over a range of (center-of-mass) energies of the Q -neutron system that decreases with increasing Q . These results provide a guide to the energy regions that experimentalists could probe which allow a controlled EFT description.

As regards future work, it would be interesting to study higher-order terms including the contributions from the droplet edge [10, 12], which are expected to scale with fractional powers of the deformation parameters. One could furthermore consider the perturbation theory relevant to Schrödinger-symmetry breaking for the large-charge expansion in the case of two spatial dimensions. In addition, while the focus of this paper has been on the large-charge two-point function, symmetry-breaking effects in three- and higher-point functions may also be of interest experimentally.

Acknowledgments

The authors would like to thank S. Aoki, J.A. Carlson, S. Gandolfi, H.W. Hammer, S. Hellerman, D.B. Kaplan, D.R. Phillips, and D.T. Son for useful discussions. This work was supported by the Swiss National Science Foundation under grant number 200021_219267. In addition, S.R.B is supported by the U. S. Department of Energy grant **DE-FG02-97ER-41014** (UW Nuclear Theory). D.O. and S.R. gratefully acknowledge support from the Yukawa Institute for Theoretical Physics at Kyoto University, as well as the from the Simons Center for Geometry and Physics at Stony Brook University, where some the research for this paper was performed.

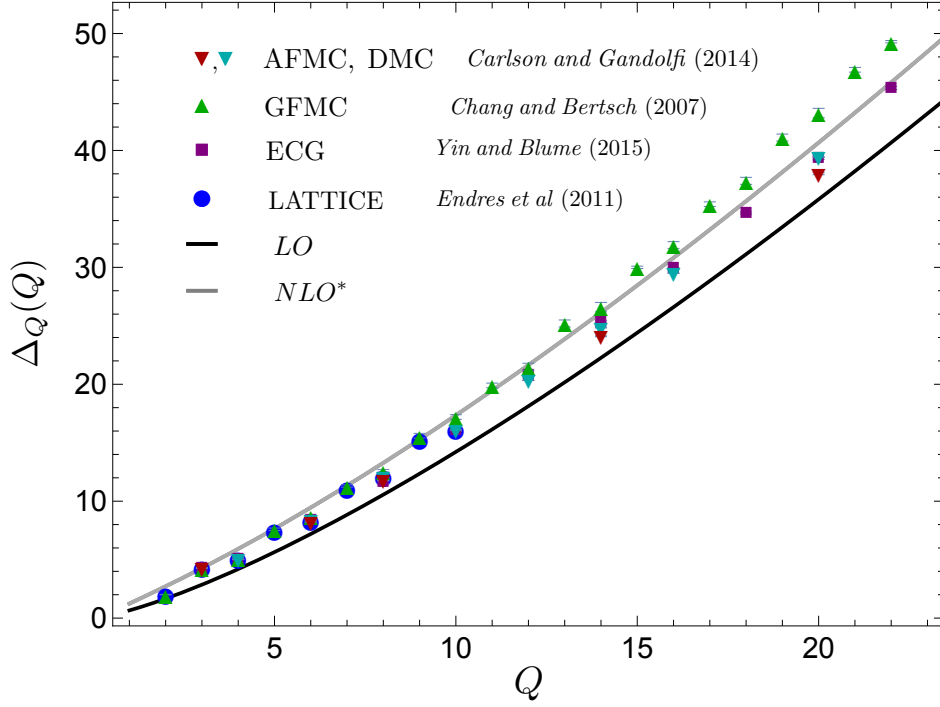


Figure 9 – Fit of DMC simulation data up to $Q = 20$, as described in the text. The solid black line is leading order in the large-charge expansion, and the gray band is the NLO fit, including the Casimir correction. The simulation data are as described in the text.

A. Improved conformal dimension

When considering applications of the large-charge EFT at low- Q values, say $Q = 3 - 6$, it is sensible to include higher-order corrections [7–9, 12, 19]. In the Schrödinger-symmetry limit, the large-charge conformal dimension to NLO takes the form

$$\Delta_Q(Q) = \frac{3^{4/3}}{4} \xi^{1/2} Q^{4/3} - 3^{2/3} \sqrt{2} \pi^2 \xi c_{\text{NLO}} Q^{2/3} + \mathcal{O}(Q^{5/9}) + \dots + \frac{1}{3\sqrt{3}} \log Q, \quad (\text{A.1})$$

where, in addition, the universal Casimir correction has been included [12]. The coefficient of the NLO term may be fit to simulation data. Fig. 9 shows simulation data up to $Q = 22$ from Green’s function MC (GFMC) [43], lattice MC [44], both diffusion MC (DMC) and auxiliary field MC (AFMC) [45], and a correlated Gaussian basis set expansion (ECG) [46]. Fitting to the AFMC data over the range $Q = 3 - 20$ one finds $c_{\text{NLO}} = -0.053715(1)$. This fit is illustrated in Fig. 9.

B. Fourier transforms

The following Fourier transforms [1, 3] are useful:

$$\begin{aligned} \int dt \int d^3\mathbf{x} \theta(t) t^{-\Delta} \exp\left(i\frac{QM\mathbf{x}^2}{2t}\right) \exp(i\mathbf{E}t - i\mathbf{p} \cdot \mathbf{x}) \\ = i^{\Delta-1} \left(\frac{2\pi}{QM}\right)^{3/2} \left(\frac{p^2}{2QM} - \mathbf{E}\right)^{\Delta-5/2} \Gamma\left(\frac{5}{2} - \Delta\right), \end{aligned} \quad (\text{B.1})$$

and

$$\begin{aligned} \int dt \int d^3\mathbf{x} \theta(t) t^{-\Delta} \log(i\lambda t) \exp\left(i\frac{QM\mathbf{x}^2}{2t}\right) \exp(i\mathbf{E}t - i\mathbf{p} \cdot \mathbf{x}) \\ = i^{\Delta-1} \left(\frac{2\pi}{QM}\right)^{3/2} \left(\frac{p^2}{2QM} - \mathbf{E}\right)^{\Delta-5/2} \Gamma\left(\frac{5}{2} - \Delta\right) \\ \times \left[\psi\left(\frac{5}{2} - \Delta\right) - \log\left(\frac{1}{\lambda} \left(\frac{p^2}{2QM} - \mathbf{E}\right)\right) \right]. \end{aligned} \quad (\text{B.2})$$

C. Variation of parameters

The differential equations studied in this paper reduce to (non-homogeneous) second-order ODES of the form

$$u''(x) + p(x)u'(x) + q(x)u(x) = f(x). \quad (\text{C.1})$$

There is a general solution of this equation, which is obtained using the *variation of parameters* [47]. Let $u_1(x)$ and $u_2(x)$ be independent solutions to the associated homogeneous problem, *i.e.* the one with $f(x) = 0$:

$$u''_{1,2}(x) + p(x)u'_{1,2}(x) + q(x)u_{1,2}(x) = 0. \quad (\text{C.2})$$

Then the general solution to the non-homogeneous problem is

$$u_G(x) = A(x)u_1(x) + B(x)u_2(x), \quad (\text{C.3})$$

where

$$A(x) = - \int^x d\xi \frac{u_2(\xi)f(\xi)}{W(\xi)} \quad B(x) = \int^x d\xi \frac{u_1(\xi)f(\xi)}{W(\xi)}, \quad (\text{C.4})$$

and $W(x)$ is the Wronskian of $u_1(x)$ and $u_2(x)$:

$$W(x) = u_1(x)u_2'(x) - u_1'(x)u_2(x). \quad (\text{C.5})$$

D. The boundary term

In the usual case it is assumed that fields vanish at spatial and temporal infinity. One consequence of this is that in perturbation theory, the solution at order n allows one to compute the action at the saddle at order $n + 1$, since there are no boundary terms. This is not the case for the action in the oscillator frame, because the couplings are time-dependent and grow exponentially at $\tilde{\tau} = \pm\infty$.

As a simple example of such a system, consider the Lagrangian

$$L = \frac{1}{2}\dot{\phi}^2 + r_0 \cosh(\omega\tilde{\tau})F(\phi) \quad (\text{D.1})$$

for $r_0 \ll 1$.

The EOM is

$$0 = \partial_t \frac{\delta L}{\delta \dot{\phi}} = \partial_{\tilde{\tau}} [\dot{\phi} + r_0 \cosh(\omega\tilde{\tau})F'(\phi)] \quad (\text{D.2})$$

$$= \ddot{\phi} + r_0 \cosh(\omega\tilde{\tau})\ddot{\phi}F'(\phi) + r_0\omega \sinh(\omega\tilde{\tau})F'(\phi). \quad (\text{D.3})$$

The solution may be written as

$$\phi = \phi_0 + r_0\phi_1, \quad (\text{D.4})$$

so the EOM at first order takes the form

$$\ddot{\phi}_0 + r_0\ddot{\phi}_1 + r_0 \cosh(\omega\tilde{\tau})\ddot{\phi}_0F'(\phi_0) + r_0\omega \sinh(\omega\tilde{\tau})F'(\phi_0) = 0, \quad (\text{D.5})$$

and, order by order,

$$\phi_0 = A\tilde{\tau} + B, \quad \phi_1 = C\tilde{\tau} + D - \frac{F'(A)}{\omega} \sinh(\omega\tilde{\tau}). \quad (\text{D.6})$$

Note that ϕ_1 does not vanish at the boundary $t = \pm T$.

The action at the saddle thus receives three contributions:

1. the LO action evaluated on the LO solution
2. the LO action evaluated on the NLO solution
3. the NLO action evaluated on the LO solution.

Contribution 2 does not vanish at the saddle due to a boundary contribution given by

$$\phi_1 \frac{\delta L}{\delta \dot{\phi}} \Big|_{-T}^T = \left(2CT - \frac{2F'(A)}{\omega} \sinh(\omega T) A \right). \quad (\text{D.7})$$

Explicitly, the action at the saddle at order $\mathcal{O}(r_0)$ reads:

$$\begin{aligned} S[\phi_0 + r_0 \phi_1] &= \int_{-T}^T d\tilde{\tau} \frac{1}{2} \dot{\phi}_0^2 + \dot{\phi}_0 \dot{\phi}_1 r_0 + \cosh(\omega t) F(\dot{\phi}_0) r_0 \\ &= \int_{-T}^T dt \frac{1}{2} A^2 + A(C - \cosh(\omega t) F'(A)) r_0 + \cosh(\omega t) F(A) r_0 \\ &= A^2 T + \left[2ACT - \frac{2AF'(A)}{\omega} \sinh(\omega T) \right] r_0 + \frac{2F(A)}{\omega} \sinh(\omega T) r_0, \end{aligned} \quad (\text{D.8})$$

which depends manifestly on the $\mathcal{O}(r_0)$ value of the field ϕ_1 .

E. Structure of the solution to the bulk EFT

It is informative to consider the general structure of the solution to the EOM, in the presence of effective-range corrections and the corresponding expansion of the action at the saddle. The Lagrange density in the oscillator frame takes the form

$$\tilde{\mathcal{L}} = -c_0 \tilde{X}^{5/2} + \frac{\mu}{\omega} \sum_{k=1} h_k r_0^k \tilde{X}^{(5+k)/2} \mu^{k/2} \cosh^k(\omega \tilde{\tau}). \quad (\text{E.1})$$

Consider a solution to the EOM of the form

$$\tilde{\theta}(\tilde{\tau}, \tilde{\nu}) = \tilde{\theta}_0(\tilde{\tau}, \tilde{\nu}) + \frac{\mu}{\omega} \sum_{k=1} (r_0 \mu^{1/2})^k \tilde{\theta}_k(\tilde{\tau}, \tilde{\nu}), \quad (\text{E.2})$$

which is an expansion around the solution $\tilde{\theta}_0(\tilde{\tau}, \tilde{\nu}) = -i\mu\tau$ of the undeformed Schrödinger problem. The EOM turns into a hierarchy for the $\tilde{\theta}_k$, where at each order there is an inhomogeneous PDE with a source of the form

$$f_k(\tilde{\tau}, \tilde{\nu}) = \varphi_k(\tilde{\nu}) \frac{d}{d\tilde{\tau}} \cosh^k(\omega \tilde{\tau}), \quad (\text{E.3})$$

where the φ_k depend on the solutions at order $k' < k$:

$$F_k(\tilde{\theta}_k, \tilde{\theta}_k'', \tilde{\theta}_k' | \tilde{\theta}_{k'}) = \varphi_k(\tilde{v}) \frac{d}{d\tilde{\tau}} \cosh^k(\omega\tilde{\tau}), \quad k' < k, \quad (\text{E.4})$$

and where F_k is by construction linear in $\tilde{\theta}_k$.

Using the fact that the RHS can be decomposed into a sum of hyperbolic sine functions,

$$\frac{d \cosh^k(\omega\tilde{\tau})}{d\tilde{\tau}} = \frac{\omega}{2^k} \sum_{l=0}^{\lfloor k/2 \rfloor} \binom{k}{l} (k-2l) \sinh((k-2l)\omega\tilde{\tau}), \quad (\text{E.5})$$

the variables can be separated by writing

$$\tilde{\theta}(\tilde{\tau}, \tilde{v}) = \sum_{l=0}^{\lfloor k/2 \rfloor} \sinh((k-2l)\omega\tilde{\tau}) B_{k,l}(\tilde{v}), \quad (\text{E.6})$$

so that the EOM turn into a hierarchy of inhomogeneous ODE for the functions $B_{k,l}$.

The transformation to the flat frame is obtained by using the identity

$$\sinh(n \operatorname{arctanh}(\omega\tau)) = \frac{1}{(1-\omega^2\tau^2)^n} \sum_{k=0}^{\lfloor n/2 \rfloor} \binom{n}{2k+1} (\tau\omega)^{2k+1} = \frac{P_n(\omega\tau)}{(1-\omega^2\tau^2)^n}. \quad (\text{E.7})$$

In what follows one can rename

$$\omega\tau = z \quad (\text{E.8})$$

in order to disentangle the parametric dependence of all the terms. Then,

$$\theta_k(z, v) = \sum_{l=0}^{\lfloor k/2 \rfloor} \frac{P_{k-2l}(z)}{(1-z^2)^{k/2-l}} B_{k,l}(v), \quad (\text{E.9})$$

and it follows that X_k takes the form

$$X_k(\tau, v) = \mu \sum_{l=0}^{\lfloor k/2 \rfloor} \frac{Q_{k,l}(z^2, v)}{(1-z^2)^{k/2+1-l}}, \quad (\text{E.10})$$

where $Q(z^2, v)$ is a polynomial in z^2 .

The analytic structure in the τ plane around the points $\pm 1/\omega$, that is $z = \pm 1$, is of special interest as this determines which terms will contribute to the final result. In the perturbative expansion of X , each term of order $\mathcal{O}(r_0^k)$ contains singularities that are either poles if k is even, or branch cuts if k is odd. The same structure, with the roles of

even and odd interchanged is found in the Lagrange density evaluated at the saddle,

$$\mathcal{L}_{\mathbb{R}} = -c_0 \frac{\mu^{5/2} L_0}{(1-z^2)^{5/2}} - \mu^{5/2} \sum_k (r_0 \sqrt{\mu})^k \sum_{l=0}^{\lfloor k/2 \rfloor} \frac{L_{k,l}(z^2, \nu)}{(1-z^2)^{(k+5)/2-l}}. \quad (\text{E.11})$$

From Eq. (5.35) it is clear that the integration measure in terms of ψ is given by

$$d\tau d^3x = \frac{1}{\omega} R_{\text{LO}}^3 (1-z^2)^{3/2} \sin^2(\psi) \cos(\psi) d\psi dz d\Omega. \quad (\text{E.12})$$

It follows that the role of poles and branch cuts is again interchanged, and

$$S_{\mathbb{R}} = -\frac{5\pi^2 c_0 \mu^4}{16\sqrt{2}\omega^4} \int_{-1}^1 \frac{dz}{1-z^2} - \frac{8\pi\sqrt{2}\mu^4}{\omega^4} \sum_k (r_0 \sqrt{\mu})^k \sum_{l=0}^{\lfloor k/2 \rfloor} \int_{-1}^1 \frac{dz}{(1-z^2)^{k/2+1-l}} \int \sin^2(\psi) \cos(\psi) d\psi L_{k,l}(z^2, \cos(\psi)). \quad (\text{E.13})$$

The integral over ψ gives a contribution that is a polynomial in z^2 , but it is still necessary to regularize the integral over z . In general these integrals will take the form

$$\mathcal{J}(n, m) = \int_{-1}^1 dz \frac{z^{2m}}{(1-z^2)^n}, \quad (\text{E.14})$$

where n is either integer (if k is even) or half-integer (if k is odd), and $m = 0, 1, \dots, \lfloor n \rfloor$.

One possible way of regularizing the $\mathcal{J}(n, m)$ is to use analytic continuation in terms of gamma functions:

$$\mathcal{J}(n, m) = \lim_{\delta \rightarrow 0} \mathcal{J}(n + \delta, m) = \lim_{\delta \rightarrow 0} \frac{\Gamma(m + 1/2) \Gamma(1 - n - \delta)}{\Gamma(3/2 + m - n - \delta)}. \quad (\text{E.15})$$

The gamma function has no zeros, but it has simple poles at negative integers. It follows that there are two possibilities:

- If n is half-integer (k is odd), the denominator has a pole for $\delta \rightarrow 0$ and the integral vanishes

$$\mathcal{J}(\mathbb{Z} + 1/2, m) = 0. \quad (\text{E.16})$$

- If n is an integer (k is even), the integral has a pole:

$$\mathcal{J}(n + \delta, m) = \frac{(-1)^n \Gamma(m + 1/2)}{\Gamma(3/2 + m - n) \Gamma(n)} \frac{1}{\delta} + \mathcal{O}(\delta^0). \quad (\text{E.17})$$

An alternative regularization is obtained by shifting the boundaries of integration:

$$\mathcal{J}(n, m) = \lim_{\epsilon \rightarrow 0} \int_{-1+\epsilon}^{1-\epsilon} dz \frac{z^{2m}}{(1-z^2)^n}. \quad (\text{E.18})$$

For n integer the integral has a logarithmic divergence in $\epsilon \rightarrow 0$, whose coefficient is precisely the same as the residue of the pole in $\delta \rightarrow 0$:

$$\int_{-1+\epsilon}^{1-\epsilon} dz \frac{z^{2m}}{(1-z^2)^n} = \frac{(-1)^n \Gamma(m + 1/2)}{\Gamma(3/2 + m - n) \Gamma(n)} \log(\epsilon) + \mathcal{O}\left(\frac{1}{\epsilon^{n-m-1}}\right) + \mathcal{O}(\epsilon^0). \quad (\text{E.19})$$

The finite terms $\mathcal{O}(\delta^0)$ and $\mathcal{O}(\epsilon^0)$ are different. This scheme dependence is however not a problem since it simply corresponds to different normalizations of the operators in the two-point function. The only physically-relevant parameter is the coefficient of the logarithm, which is determined unambiguously.

This structure holds for the bulk terms. However, there are contributions due to the fact that the density decreases sharply at the droplet edge. There are thus boundary effects that can lead to new corrections that scale differently. In the study of the NLO corrections (Section 5), it was found that the size of the droplet is reduced by an amount proportional to $r_0^{2/3}$, which translates into a correction of $\mathcal{O}(r_0^{7/3})$. The appearance of new fractional powers (and logarithmic terms) has already been observed in conjunction with boundary effects in the large-charge expansion in the undeformed Schrödinger-symmetric case [10, 12].

Up to this point the results have been expressed as functions of the parameter μ . In Section 5.5 the relationship between μ and Q was found to be independent of r_0 at NLO because of the cancellation of all the $\mathcal{O}(r_0)$ terms. However, the same cancellation must occur at all orders. Each power of r_0 in the expression of the density ρ is accompanied by powers of $(1 - \omega^2 \tau^2)$. All these terms have to cancel separately already on the LHS of the differential form of the continuity equation (5.47), because there is no such τ dependence on the RHS. The conclusion is therefore that the expression of μ as function of Q in Eq. (5.54) is valid at all orders in r_0 : $(\mu/\omega)^3 = 3\xi^{3/2} Q$.

References

- [1] H.-W. Hammer and D. T. Son. *Unnuclear physics*. *Proc. Nat. Acad. Sci.* 118 (2021), e2108716118. DOI: 10.1073/pnas.2108716118. arXiv: 2103.12610 [nucl-th].
- [2] T. Schaefer and G. Baym. *From nuclear to unnuclear physics* (Sept. 2021). DOI: 10.1073/pnas.2113775118. arXiv: 2109.06924 [nucl-th].
- [3] E. Braaten and H.-W. Hammer. *Point production of a nonrelativistic unparticle recoiling against a particle*. *Phys. Rev. D* 107.3 (2023), p. 034017. DOI: 10.1103/PhysRevD.107.034017. arXiv: 2301.04399 [hep-th].
- [4] S. D. Chowdhury, R. Mishra, and D. T. Son. *Applied nonrelativistic conformal field theory: scattering-length and effective-range corrections to unnuclear physics* (Sept. 2023). arXiv: 2309.15177 [hep-th].
- [5] H. Georgi. *Unparticle physics*. *Phys. Rev. Lett.* 98 (2007), p. 221601. DOI: 10.1103/PhysRevLett.98.221601. arXiv: hep-ph/0703260.
- [6] M. Greiter, F. Wilczek, and E. Witten. *Hydrodynamic Relations in Superconductivity*. *Mod. Phys. Lett. B* 3 (1989), p. 903. DOI: 10.1142/S0217984989001400.
- [7] D. T. Son and M. Wingate. *General coordinate invariance and conformal invariance in nonrelativistic physics: Unitary Fermi gas*. *Annals Phys.* 321 (2006), pp. 197–224. DOI: 10.1016/j.aop.2005.11.001. arXiv: cond-mat/0509786.
- [8] S. Favrod, D. Orlando, and S. Reffert. *The large-charge expansion for Schrödinger systems*. *JHEP* 12 (2018), p. 052. DOI: 10.1007/JHEP12(2018)052. arXiv: 1809.06371 [hep-th].
- [9] S. M. Kravec and S. Pal. *The Spinful Large Charge Sector of Non-Relativistic CFTs: From Phonons to Vortex Crystals*. *JHEP* 05 (2019), p. 194. DOI: 10.1007/JHEP05(2019)194. arXiv: 1904.05462 [hep-th].
- [10] S. Hellerman and I. Swanson. *Droplet-Edge Operators in Nonrelativistic Conformal Field Theories* (Oct. 2020). arXiv: 2010.07967 [hep-th].
- [11] V. Pellizzani. *Operator spectrum of nonrelativistic CFTs at large charge*. *Phys. Rev. D* 105.12 (2022), p. 125018. DOI: 10.1103/PhysRevD.105.125018. arXiv: 2107.12127 [hep-th].
- [12] S. Hellerman, D. Orlando, V. Pellizzani, S. Reffert, and I. Swanson. *Nonrelativistic CFTs at large charge: Casimir energy and logarithmic enhancements*. *JHEP* 05 (2022), p. 135. DOI: 10.1007/JHEP05(2022)135. arXiv: 2111.12094 [hep-th].
- [13] S. Hellerman et al. *The unitary Fermi gas at large charge and large N* (Nov. 2023). arXiv: 2311.14793 [hep-th].
- [14] Y. Nishida and D. T. Son. *Nonrelativistic conformal field theories*. *Phys. Rev. D* 76 (2007), p. 086004. DOI: 10.1103/PhysRevD.76.086004. arXiv: 0706.3746 [hep-th].
- [15] D. Orlando, S. Reffert, and F. Sannino. *Near-Conformal Dynamics at Large Charge*. *Phys. Rev. D* 101.6 (2020), p. 065018. DOI: 10.1103/PhysRevD.101.065018. arXiv: 1909.08642 [hep-th].
- [16] D. Orlando, V. Pellizzani, and S. Reffert. *Near-Schrödinger dynamics at large charge*. *Phys. Rev. D* 103.10 (2021), p. 105018. DOI: 10.1103/PhysRevD.103.105018. arXiv: 2010.07942 [hep-th].
- [17] S. Hellerman, D. Orlando, S. Reffert, and M. Watanabe. *On the CFT Operator Spectrum at Large Global Charge*. *JHEP* 12 (2015), p. 071. DOI: 10.1007/JHEP12(2015)071. arXiv: 1505.01537 [hep-th].

- [18] L. A. Gaumé, D. Orlando, and S. Reffert. *Selected topics in the large quantum number expansion*. *Phys. Rept.* 933 (2021), pp. 1–66. DOI: 10.1016/j.physrep.2021.08.001. arXiv: 2008.03308 [hep-th].
- [19] S. R. Beane, D. Orlando, and S. Reffert. *Exact evaluation of large-charge correlation functions in nonrelativistic conformal field theory*. *Phys. Rev. D* 110.2 (2024), p. 025011. DOI: 10.1103/PhysRevD.110.025011. arXiv: 2403.18898 [hep-th].
- [20] O. Bergman and G. Lozano. *Aharonov-Bohm scattering, contact interactions and scale invariance*. *Annals Phys.* 229 (1994), pp. 416–427. DOI: 10.1006/aphy.1994.1013. arXiv: hep-th/9302116.
- [21] P. Maris, J. P. Vary, S. Gandolfi, J. Carlson, and S. C. Pieper. *Properties of trapped neutrons interacting with realistic nuclear Hamiltonians*. *Phys. Rev. C* 87.5 (2013), p. 054318. DOI: 10.1103/PhysRevC.87.054318. arXiv: 1302.2089 [nucl-th].
- [22] F. M. Marqués and J. Carbonell. *The quest for light multineutron systems*. *Eur. Phys. J. A* 57.3 (2021), p. 105. DOI: 10.1140/epja/s10050-021-00417-8. arXiv: 2102.10879 [nucl-ex].
- [23] Z. H. Yang et al. *Study of multi-neutron systems with SAMURAI spectrometer*. *Springer Proc. Phys.* 238 (2020), pp. 529–534. DOI: 10.1007/978-3-030-32357-8_87. arXiv: 1903.11256 [nucl-ex].
- [24] Nakamura, T. “Pure-neutron nuclei – current and future”. HaloWeek’24 - nuclei at and beyond the driplines. 2024. URL: https://indico.cern.ch/event/1319370/contributions/5985670/attachments/2876623/5037885/Nakamura_halo_week_4n_pub.
- [25] M. Duer et al. *Observation of a correlated free four-neutron system*. *Nature* 606.7915 (2022), pp. 678–682. DOI: 10.1038/s41586-022-04827-6.
- [26] D. B. Kaplan, M. J. Savage, and M. B. Wise. *A New expansion for nucleon-nucleon interactions*. *Phys. Lett. B* 424 (1998), pp. 390–396. DOI: 10.1016/S0370-2693(98)00210-X. arXiv: nucl-th/9801034.
- [27] D. B. Kaplan, M. J. Savage, and M. B. Wise. *Two nucleon systems from effective field theory*. *Nucl. Phys. B* 534 (1998), pp. 329–355. DOI: 10.1016/S0550-3213(98)00440-4. arXiv: nucl-th/9802075.
- [28] S. R. Beane and M. J. Savage. *Rearranging pionless effective field theory*. *Nucl. Phys. A* 694 (2001), pp. 511–524. DOI: 10.1016/S0375-9474(01)01088-0. arXiv: nucl-th/0011067.
- [29] J. Carlson, S. Gandolfi, K. E. Schmidt, and S. Zhang. *Auxiliary-field quantum Monte Carlo method for strongly paired fermions*. *Phys. Rev. A* 84 (6 2011), p. 061602. DOI: 10.1103/PhysRevA.84.061602. URL: <https://link.aps.org/doi/10.1103/PhysRevA.84.061602>.
- [30] A. Bulgac and G. F. Bertsch. *Collective Oscillations of a Trapped Fermi Gas near the Unitary Limit*. *Phys. Rev. Lett.* 94 (2005), p. 070401. DOI: 10.1103/PhysRevLett.94.070401. arXiv: cond-mat/0404687.
- [31] U. van Kolck. *Unitarity and Discrete Scale Invariance*. *Few Body Syst.* 58.3 (2017), p. 112. DOI: 10.1007/s00601-017-1271-9.
- [32] M. M. Forbes, S. Gandolfi, and A. Gezerlis. *Effective-Range Dependence of Resonantly Interacting Fermions*. *Phys. Rev. A* 86 (2012), p. 053603. DOI: 10.1103/PhysRevA.86.053603. arXiv: 1205.4815 [cond-mat.quant-gas].
- [33] S. Y. Chang, V. R. Pandharipande, J. Carlson, and K. E. Schmidt. *Quantum Monte Carlo Studies of Superfluid Fermi Gases*. *Phys. Rev. A* 70 (2004), p. 043602. DOI: 10.1103/PhysRevA.70.043602. arXiv: physics/0404115.
- [34] C. R. Hagen. *Scale and conformal transformations in galilean-covariant field theory*. *Phys. Rev. D* 5 (1972), pp. 377–388. DOI: 10.1103/PhysRevD.5.377.

- [35] U. Niederer. *The maximal kinematical invariance group of the free Schrodinger equation*. *Helv. Phys. Acta* 45 (1972), pp. 802–810. DOI: 10.5169/seals-114417.
- [36] M. Henkel. *Schrodinger invariance in strongly anisotropic critical systems*. *J. Statist. Phys.* 75 (1994), pp. 1023–1061. DOI: 10.1007/BF02186756. arXiv: hep-th/9310081.
- [37] D. T. Son, M. Stephanov, and H.-U. Yee. *Fate of multiparticle resonances: From Q-balls to He3 droplets*. *Phys. Rev. A* 106.5 (2022), p. L050801. DOI: 10.1103/PhysRevA.106.L050801. arXiv: 2112.03318 [nucl-th].
- [38] S. M. Kravec and S. Pal. *Nonrelativistic Conformal Field Theories in the Large Charge Sector*. *JHEP* 02 (2019), p. 008. DOI: 10.1007/JHEP02(2019)008. arXiv: 1809.08188 [hep-th].
- [39] W. D. Goldberger, Z. U. Khandker, and S. Prabhu. *OPE convergence in non-relativistic conformal field theories*. *JHEP* 12 (2015), p. 048. DOI: 10.1007/JHEP12(2015)048. arXiv: 1412.8507 [hep-th].
- [40] L. Platter, C. Ji, and D. R. Phillips. *Range Corrections to Three-Body Observables near a Feshbach Resonance*. *Phys. Rev. A* 79 (2009), p. 022702. DOI: 10.1103/PhysRevA.79.022702. arXiv: 0808.1230 [cond-mat.other].
- [41] S. Gandolfi, G. Palkanoglou, J. Carlson, A. Gezerlis, and K. E. Schmidt. *The 1S0 Pairing Gap in Neutron Matter*. *Condens. Mat.* 7.1 (2022), p. 19. DOI: 10.3390/condmat7010019. arXiv: 2201.01308 [nucl-th].
- [42] J. Golak et al. *Radiative pion capture in ^2H , ^3He and ^3H* . *Phys. Rev. C* 98.5 (2018), p. 054001. DOI: 10.1103/PhysRevC.98.054001. arXiv: 1807.07235 [nucl-th].
- [43] S. Y. Chang and G. F. Bertsch. *Unitary Fermi gas in a harmonic trap*. *Phys. Rev. A* 76 (2007), p. 021603. DOI: 10.1103/PhysRevA.76.021603. arXiv: physics/0703190.
- [44] M. G. Endres, D. B. Kaplan, J.-W. Lee, and A. N. Nicholson. *Lattice Monte Carlo calculations for unitary fermions in a harmonic trap*. *Phys. Rev. A* 84 (2011), p. 043644. DOI: 10.1103/PhysRevA.84.043644. arXiv: 1106.5725 [hep-lat].
- [45] J. Carlson and S. Gandolfi. *Predicting Energies of Small Clusters from the Inhomogeneous Unitary Fermi Gas*. *Phys. Rev. A* 90.1 (2014), p. 011601. DOI: 10.1103/PhysRevA.90.011601. arXiv: 1406.3591 [cond-mat.quant-gas].
- [46] X. Y. Yin and D. Blume. *Trapped unitary two-component Fermi gases with up to ten particles*. *Physical Review A* 92.1 (July 2015). ISSN: 1094-1622. DOI: 10.1103/physreva.92.013608. URL: <http://dx.doi.org/10.1103/PhysRevA.92.013608>.
- [47] J.-L. Lagrange. “Sur la théorie générale de la variation des constantes arbitraires dans tous les problèmes de la mécanique”. In: *Oeuvres de Lagrange*. Ed. by J.-A. Serret. Vol. 6. Gauthier-Villars, 1873, pp. 771–805. URL: <https://gallica.bnf.fr/ark:/12148/bpt6k229225j/f773>.